CRS
Italy Local Chapter

Design and Industrial Development of Advanced Drug Delivery Systems

Thematic Workshop of Controlled Release Society Italian Chapter

University of Pavia
Palazzo Centrale
Via Strada Nuova 65, Pavia
November 21st – 23rd, 2013

Abstract Book - Poster

Organizing committee:

Prof. Pietro Matricardi
Prof. Ida Genta
Dr. Rossella Dorati
Dr. Barbara Colzani
Dr. Giuseppe Tripodo

Scientific committee:

Prof. Paolo Caliceti
Prof. Bice Conti
Prof. Elias Fattal
Prof. Gennara Cavallaro
Dr. Giuseppe De Rosa

ALFA TEST

Qi technologies

CAPSUGEL®

Provider:
Ufficio ECM
Dipartimento di Scienze del Farmaco
Università degli Studi di Pavia

Responsabile: Prof. Tiziana Modena
Tel. 0382 987384 - Cell. 339 8866844
Fax 0382 987931 – 0382 422975
segreteria@ecmunipv.it

EVONIK INDUSTRIES

Ordine provinciale dei farmacisti di Pavia

APTALIS™

BÜCHI SWITZERLAND

INDEX

HIGH THROUGHPUT DESIGN OF POLYAMIDOAMINE NANOPARTICLES FOR TARGET THERAPIES

S. Argentiere, A. Tocchio, C. Cella, E. Rossi, F. Martello, I. Gerges, C. Lenardi, P. Milani

Fondazione Filarete, Viale Ortles 22/4, 20139 Milano

Synthetic polymers are receiving increasing attention in drug/gene delivery because their rational design allow to optimize their functional properties and thereby the release kinetic profile.

One attractive class of synthetic polymers to design nanosized carriers is polyamidoamines (PAAs), which are obtained by Michael-type polyaddition of primary or bis secondary amines to bisacrylamides.[1]

Besides their biodegradability, PAA nanocarriers (NCs) are particularly attractive for target therapies because different bioactive molecules can be incorporated in their polymer backbone by covalent attachment during the synthetic process.

Recently, polyamidoamines containing 4-aminobutylguanidine (ABG) have been reported to mimic the tripeptide sequence Arg-Gly-Asp (RGD),[2] which has shown to be successful for selective targeting of tumor cells via the integrin receptors.[3] Unlike the RGD-modified NCs, this approach does not require complex synthetic procedures and high production costs.

Further, to date PAA nanoparticles have been mainly prepared by mixing oppositely charged drug and polymers that interact by electrostatic attraction. Several PAAs nanoparticles have been prepared by self-assembly of PAAs, which are positively charged at physiological pH, and proteins with isoelectric point higher than 7.4.[2,4]

However, these non-covalent nanoassemblies suffer from limitations such as polidispersity and instability. Since they are known to aggregate after 24-48 h, their capability to get the target site could be reduced as well.

Here, we report an innovative method to synthesize PAA nanocarriers containing ABG as RGD-like units. To this aim, PAA oligomers containing ABG were crosslinked with human serum albumin (HSA) and methacrylate polymers in the presence of UV light (UV lamp B-100AP, UVP LLC, 365 nm, 10 mW/cm2). The covalent linking of PAA with methacrylate groups and RGD-mimetic moieties allowed to obtain biofunctionalized UV-photocrosslinkable NCs. The morphological characterization of PAA NCs was performed by Dynamic Light Scattering (DLS, Malvern ZS90) and Scanning Electron Microscopy (SEM, Zeiss Sigma, Fig. 1)

This synthetic method has the advantage of providing stable NCs (up to 1 month) without requiring sonication or organic solvents, which are both harmful for proteins and peptides and are usually employed for preparing nanoparticles by double emulsion technique.

As a proof of concept, β-galactosidase was encapsulated into the PAA NCs and the enzymatic activity measured using O-nitrophenyl-β-D-galactoside (ONPG) as substrate.

In conclusion, in this work we describe the design and preparation of biodegradable PAA nanocarriers, as efficient vectors for controlled delivery of bioactive molecules. PAA nanoparticles are fabricated by UV crosslinking of PAA linear oligomers with HSA and methacrylate groups. Notably, since this methods exploits UV-induced crosslinking, it can be easily scaled up for industrial applications.

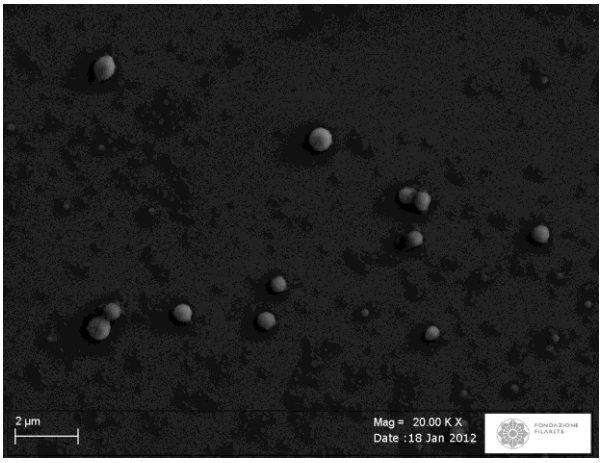

Fig. 1. SEM image of PAA NCs.

References

[1] Ferruti P., Marchisio M. A., Duncan R., Macromol. Rapid Commun. 2002, 23, 332-355.

[2] Cavalli R., Bisazza A., Sessa R., Primo L., Fenili F., Manfredi A., Ranucci E., Ferruti P., Biomacromolecules. 2010, 11(10), 2667-74.

[3] Parkhouse S. M. Garnett M. C., Chan W. C., Bioorganic & Medicinal Chemistry 2008, 16, 6641-6650.

[4] Couè G., Engbersen J. F. J., J.Control. Rel. 2011, 152, 90-98.

NANOTECHNOLOGY AND INFECTIONS: VANCOMYCIN–LOADED NANOBUBBLES AS ULTRASOUND-TRIGGERED ANTIBACTERIAL DELIVERY SYSTEM

Monica Argenziano[1], Mauro Prato[2], Amina Khadjavi[2], Giuliana Banche[3], Caterina Guiot[2], Roberta Cavalli[1]
[1]Dipartimento di Scienza e Tecnologia del Farmaco, Università di Torino, Torino, Italy
[2]Dipartimento di Neuroscienze, Università di Torino, Torino, Italy
[3]Dipartimento di Scienze della Sanità Pubblica e Pediatriche, Università di Torino, Torino, Italy

Vancomycin is a glycopeptide antibiotic used in the treatment of infections caused by Gram-positive bacteria, which are unresponsive to other less toxic antibiotics; particularly it is been the most reliable therapeutic agent against infections caused by meticillin-resistant *Staphylococcus aureus* (MRSA). This drug is a molecule with high molecular weight, soluble in water, poorly absorbed from the gastrointestinal tract and its systemic administration can be associated with severe adverse effects. Moreover, the drug shows poor intracellular penetration [1]. These limitations might be overcome by delivering vancomycin within a nanocarrier. An innovative approach would be the use of physical external stimuli, such as ultrasound (US), to enhance drug penetration through biological barriers using US-resonant bubbles as carriers.

Nanobubbles are spherical core/shell structures filled by a gas, with sizes lower than 1 µm. They have gained an increasing attention for drug delivery, because they can be loaded with drugs and genes for targeted release, due to their potential to be activated by the presence of ultrasound [2,3]. A strategy for obtaining stable bubble systems is the use of gas not soluble in water (e.g. perfluorocarbons). Here, for the development of nanobubbles we choose perfluoropentane, a perfluorocarbon liquid at room temperature (boiling point 29 °C). We prepare nanoemulsion containing liquid perfluoropentane, that convert into bubbles in the presence of US. The phenomenon called acoustic droplet vaporisation (ADV) allows nanodroplets to be converted into larger bubbles following a pulse of US, permitting the liquid-to-gas transition within the bubble core [4].

The aim of this work was to prepare dextran nanobubbles for the local delivery of vancomycin for cutaneous infectious diseases. Topical treatment of skin infections is advantageous due to the direct delivery of drugs to the site of action reducing the doses and unwanted effects at other non-targeted tissue [5].

Dextran NBs were prepared according to the method previously reported [6]. Vancomycin loaded nanobubbles (VLNBs) were obtained adding vancomycin aqueous solution (1 mg/ml, pH 3.5) to the preformed NBs. Blank nanobubbles (NBs) were prepared in the absence of VA. Fluorescent formulations were obtained adding 6-coumarin in the gas core. The VLNBs were then purified by dialysis to eliminate unbounded molecules.

Nanobubbles, either blank or drug-loaded, were *in vitro* characterized by size and surface charge determination, drug loading, TEM analyses and drug release studies in the presence and in the absence of ultrasound (2.5 MHz, 5 min). The stability of the formulations was evaluated determining morphology and sizes over time and after insonation. Preliminary permeation studies were carried out using a purposely modified Franz-cell; the permeation of vancomycin through pig skin was evaluated after insonation (2.5 MHz, 10 min). Antibacterial efficiency on methicillin-resistant *Staphylococcus Aureus* (MRSA) of vancomycin-loaded nanobubbles was *in vitro* tested. Cytotoxicity studies on human keratinocytes (HaCaT cell line) were also carried out to evaluate the formulation safety.

The nanobubbles showed sizes less than 400 nm, spherical shape and a negative surface charge. Dextran nanobubbles were able to load vancomycin with an encapsulation efficiency of about 86%. The stability of the formulations was confirmed by morphological and size analyses, over time and after insonation. A prolonged release kinetics was demonstrated without initial burst effect; the application of ultrasound enhance the drug release. Vancomycin accumulated in the skin reaching more than 300 µg/cm^2 after insonation. VLNBs proved to be effective in bacterial killing without showing toxic effects on human keratinocytes. Based on these results, vancomycin properly formulated in nanobubbles, might be a promising strategy for the topical treatment of MRSA infection.

References

[1] Vandecasteele S. J., De Vriese A.S., Tacconelli E., J Antimicrob Chemother 2013, 68, 743-748;
[2] Bisazza A., Cavalli R., Soft Matter 2011,7, 10590;
[3] S. Sirsi and M. Borden, Bubble Sci Eng Technol. 2009, 1(1-2): 3–17;
[4] Kripfgans, O.D. et al, J. Acoust. Soc. Am., 116, 272-281
[5] Prabhu P., Patravale V., Joshi M., Current Nanoscience, 2012, 8, 491-503;
[6] Cavalli R., Guiot C., Trotta M., Int J Pharm. 2009;381:160-5

LIPOSOMAL siRNA FOR PEL CANCER

Daniela Belletti[1], *Giovanni Riva*[2], *Giovanni Tosi*[1], *Ivana Lagreca*[2], *Patrizia Barozzi*[2], *Adriana Mattiolo*[3], *Elena Negri*[3], *Laura Lignitto*[3] *Flavio Forni*[1], *Mario Luppi*[2], *Luigi Chieco-Bianchi*[4], *Maria Angela Vandelli*[1], *Maria Luisa Calabrò*[3], *Barbara Ruozi*[1]

[1] *Department of Life Sciences, University of Modena and Reggio Emilia, Italy;*[2] *Department of Medical and Surgical Sciences, Section of Hematology, University of Modena and Reggio Emilia, Italy;*[3] *Immunology and Molecular Oncology, Veneto Institute of Oncology, IOV – IRCCS, Padova, Italy;*[4] *Department of Surgery, Oncology and Gastroenterology, University of Padova, Italy*

The clinical efficacy of conventional anticancer chemotherapy is typically hampered by high systemic toxicity and low drug concentration levels in neoplastic tissue, often resulting in a dismal therapeutic index of these drugs. Thus, tumor-specific delivery of anticancer drugs by means of "targeted nanocarriers" (oncologic nanomedicine) is being investigated as an attractive approach to enhance antitumoral effects together with the reduction of side effects possibly offering a radical improvement in the treatment of oncologic patients. In this contest, we propose an innovative target strategies to improve the treatment of human herpesvirus 8 (HHV8)-associated primary effusion lymphoma (PEL). Primary effusion lymphoma (PEL) is a rare HIV-associated non-Hodgkin's lymphoma (NHL) that accounts for approximately 4% of all HIV-associated NHL. PEL generally occurs as a lymphomatous effusion in serous cavities such as the pleural space, pericardium, and peritoneum. PEL's treatment generally involves the combination of chemotherapy and antiretroviral therapy, but the prognosis for patients is generally poor, with a median survival time ~~of~~ around 6 months [1]. Recently, small interfering RNAs (siRNAs), able to knock-down viral oncogenic proteins, were shown to induce efficient PEL cell apoptosis in vitro and PEL regressions in mice treated with intracavitary injection of lentiviral vectors expressing siRNA precursors [2].

Cationic and stealth-cationic liposomes were optimized to deliver specific siRNAs to knock-down novel molecular targets (HHV8-encoded microRNAs, viral oncogenic proteins, or host transcription factors) recently identified by our collaborators, with relevant functions in PEL pathogenesis [3]. We are presently testing the delivery efficiency and the administration stability of these lipoplexes. Antineoplastic activity is being demonstrated *in vitro* using different PEL-derived cell lines and *in vivo* on a previously established PEL mouse model [4].

The results demonstrated the ability of lipoplexes to stabilize and deliver high amount of siRNAs into PEL cells. Experiments using a mixture of siRNAs targeting a specific cellular gene, showed a remarkable dose-dependent apoptosis, measured by annexin-V/PI staining, in lipoplexes-transfected PEL cells. *In vivo* delivery of these therapeutic siRNAs significantly increased the survival time of treated mice compared with control treatment (log-rank test, lipoplexes vs empty liposomes, p=0.002), indicating that lipoplexes exerted a significant antineoplastic activity. The empty carriers were not toxic in control mice and did not delay PEL development respect untraeted mice. This is the first *in vivo* application of siRNA delivery in PEL treatment by using non-viral vectors. Liposomes/siRNA complexes that provides an efficient silencing of the target gene and a great reduction in toxicity may therefore be considered as the basis for the development of useful short interfering RNA therapeutics to treat PEL tumor. Moreover, we identified a target gene whose suppression exerts a relevant tumoricidal activity on PEL cells *in vitro* and *in vivo*, opening new perspectives for PEL treatment.

Financial Support by the PRIN 2009.

References:

1. Chen, Y.B., et al.: Oncologist. 2007, 12(5):569-76.
2. Godfrey, A., et al.*: Blood* **2005**, 105: 2510-2518.
3. Luppi, M, et al.: *Leukemia* **2005**,19: 473–476..
4. Calabrò, ML, et al. : *Blood.* **2009**,113: 4525-4533.

ATOMIC FORCE MICROSCOPY ON GOLD NANOPARTICLES

[1]B. Albertini, [2]F. Rocchi, [3]L. Tarpani, [2]A. Calandra, [4]A. Di Michele, [3]L. Latterini, [2]N. Forini, [1]P.Blasi

[1]Dipartimento di Chimica e Tecnologia del Farmaco, [2]Dipartimento di Scienze Chirurgiche, Radiologiche e Odontostmatologiche, [3]Dipartimento di Chimica, [4]Dipartimento di Fisica; Università degli Studi di Perugia

Compared to other microscopic techniques, such as scanning electron microscopy and transmission electron microscopy (TEM), atomic force microscopy (AFM) presents several advantages like the possibility to determine surface topography with subnanometre resolution [1].

Due to the importance of nanoparticle size, shape, and surface topography in biodistribution and toxicity, it is essential to have means to determine these features with extreme precision and reproducibility [2].

The aim of this work was to evaluate the performances (resolution) of AFM in order to optimize a protocol for the characterization of gold nanoparticles (AuNPs) applicable in theranostics.

AuNPs were prepared reducing Au^{3+} ($HAuCl_4$) to Au^0 at 50°C using, in the first preparation, sodium citrate as reducing and stabilizing agent (Sample A) and, in the second, sodium citrate as reducing agent and poly(vinyl alcohol) as stabilizer (Sample B). AuNP particle size was determined using dynamic light scattering. Sample A showed two populations with a mean hydrodynamic diameter (D_H) of 2.6±0.6 nm (99.9%, v/v) and of 22.1±5.70 nm (0.1%, v/v). In sample B, the two populations had a D_H of 2.2±0.0 nm (99.9%, v/v) and of 37.9±1.30 nm (0.1%, v/v). From TEM analysis it was possible to confirm the particle size and to hypothesize the AuNP spherical shape.

The two samples were characterized using an AFM Solver Pro, NT-MDT. AuNP suspensions were deposited in mica slide and the continuous phase (water) was evaporated overnight. Samples were analysed in tapping mode to avoid particle dragging. The same sample was scanned at progressively higher magnifications (scanned areas: 7X7 μm^2, 5X5 μm^2, 2X2 μm^2, 1X1 μm^2 and 0.5X0.5 μm^2) and images were elaborated using the WSxM 5.0 software.

To evaluate AFM performance (lateral resolving power), the same frame was scanned 3 times at each magnification, the minimal distance between the same two distinguishable objects was estimated and the standard deviation calculated. The mean value obtained for each sample characterizes inversely the performance of the instrument. From the different measurements performed, sample A was resolved at all the magnifications investigated, while sample B was not resolved for the two highest magnifications (**Tables 1 and 2**; **Fig. 1**). This is probably due to the presence of PVA that flakes following multiple scans (tip-sample interactions). Anyhow, the resolving power did not increase over a certain magnification (2X2 μm^2).

Then, the possibility of using the profile function to acquire information of a particular detail reduces with the increase of magnification. In addition, particular attention has to be paid when analysing objects covered by a polymer shell.

The data obtained from the different scans suggest that the performance of the instrument decreases slightly at higher magnifications.

Table 1. Measurements of the distance between 2 AuNPs of Sample A.

Measure	Distance (nm)
1	72.008
2	69.372
3	77.952
4	66.884
5	71.509
6	71.377
7	76.035
8	69.589
9	69.026
10	68.883
11	76.613
12	77.661
13	73.585
14	66.137
15	71.661
Mean (lateral resolving power)	**71.886**
Standard deviation	**3.7**

Table 2. Measurements of the distance between 2 AuNPs of Sample B.

Measure	Distance (nm)
1	120.341
2	119.181
3	118.161
4	121.268
5	109.807
6	116.803
7	104.508
8	123.397
9	109.366
Mean (lateral resolving power)	**115.870**
Standard deviation	**6.4**

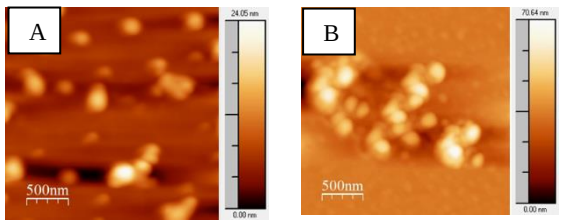

Figure 1. AFM images of sample A and sample B.

References

[1] Jalili N et al, Mechatronics 14, 907 (2004);
[2] Xie J et al, Adv. Drug Deliv. Rev. 62, 1064 (2010).

GOLD NANOPARTICLE SIZE EVALUATION USING DIFFERENT METHODS

B. Albertini, S.M.L. Greco, E. Cassetti, A. Schoubben, P. Blasi, M. Ricci

Dipartimento di Chimica e Tecnologia del Farmaco, Università degli Studi di Perugia, Perugia (Italy)

Gold nanoparticles (AuNPs) have attracted considerable interest in the last years for their potential biomedical applications as theranostic agent [1]. AuNP optical properties, such as surface plasmon resonance, are the key features for their application in diagnostics. While working with nanomaterials, particle size and the developed surface area are of paramount importance since it correlates somehow with biodistribution, cellular uptake and toxicity. AuNP *in vivo* biodistribution, after intravenous administration, has been found to depend on particle size. For instance, 15 nm AuNPs were detected in all tissues, including liver, kidney and brain vessel endothelia cells, while 200 nm AuNPs were found in minute amount in brain, stomach and pancreas [2]. The toxicity of AuNPs in rodents also depended on the particle size: small (i.e., 3-5 nm) and large size (i.e., 50-100 nm) nanoparticles (NPs) were not toxic, while medium size (i.e., 8, 12, 17, 37 nm) induced severe sickness and loss of weight [3].

Although extremely important, NP size estimation is often overlooked and different methods provide diverse results. The aim of this work is to compare the particle size estimated using different methods. Dynamic light scattering (DLS) (NICOMP 380 ZLS, NICOMPTM, California, USA) and image analysis of transmission electron microscopy (TEM) (Philips EM 400T microscope, Holland, EU) photomicrograph were evaluated. To determine AuNP size from TEM photomicrograph, two softwares were employed: ImageJ and MatLab. ImageJ is a Java-based open source software developed at the National Institutes of Health. MatLab is a numerical computing environment characterized by high programming language. DLS estimates mean hydrodynamic equivalent diameter (D_H), while from image analysis, NP particle size can be expressed as mean projected area diameter (D_P).

AuNPs were prepared by reducing Au^{3+} (from $HAuCl_4$) to Au^0 with sodium citrate as reducing and stabilizing agent at different temperatures (100°C, sample 1; 75°C, sample 2; 50°C, sample 3). From the DLS analyses it can be noted that AuNPs prepared at 75 and 50°C were smaller than NPs synthesized at 100°C, with the most abundant population around 2-3 nm (**Table 1**). Particle mean D_P determined using ImageJ and MatLab was slightly different from DLS measurements (**Tables 1 and 2**). Small differences could also be observed elaborating the images with the two softwares (**Table 2**). The latest may be due to the diverse number of particles sized and software differences. Once optimized the script, MatLab analyses automatically most of the particles on the pictures. On the contrary, analysis with ImageJ was more tedious (due to the need of manual interventions) and not all the pictures could be analysed. Even though generally smaller, in the case of 10-30 nm particles, image analysis and DLS provided similar results (**Tables 1 and 2**).

Table 1. Particle size obtained by dynamic light scattering analysis.

Sample	Equivalent diameter	Population 1	Population 2
		Mean D_H ±s.d.(nm) [abundance %]	Mean D_H ± s.d. (nm) [abundance %]
1	Intensity	17.7±3.10 [53.9%]	67.1±1.90 [46.1%]
	Number	13.5 ± 2.10 [99.99%]	60.1±0.07 [0.01%]
	Volume	15.6±1.60 [98.2%]	61.6±2.10 [1.80%]
2	Intensity	2.3±0.0 [17.3%]	28.7±4.50 [82.7%]
	Number	2.2 ± 0.0 [99.6%]	22.8 ± 0.20 [0.4%]
	Volume	2.2±0.0 [99.8%]	26.7±1.40 [0.20%]
3	Intensity	2.7±0.6 [39.7%]	28.8±5.90 [60.3%]
	Number	2.4±0.4 [99.99%]	21.1±3.10 [0.01%]
	Volume	2.6±0.6 [99.9%]	22.1±5.70 [0.10%]

Table 2. Particle size obtained by image analysis.

Sample	MatLab		ImageJ	
	Mean D_P ±s.d. (nm)	n.*	Mean D_P ±s.d. (nm)	n.*
1	15.7±2.20	810	15.2±5.40	113
2	16.2±2.70	3322	18.4±3.40	309
3	14.7±3.30	639	14.0±2.50	48

* Number of NP analysed.

With the experimental set up employed, image analysis failed to detect and measure 2-3 nm particles (**Fig. 1**). Single particles (2-3 nm) were formed by few pixels and the photograph background made extremely difficult the elaboration.

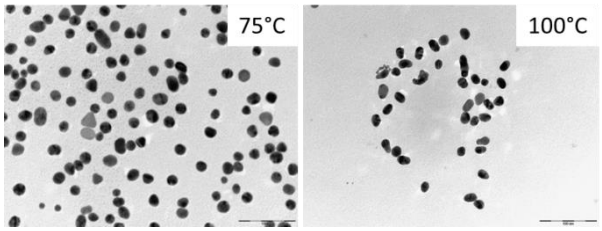

Figure 1. TEM photomicrograph of AuNPs prepared at 75 and 100°C.

Concerning the different results obtained with the two techniques, it is important to consider that DLS estimates the mean D_H (diameter of a sphere with the same translational diffusion coefficient as the particle in the same fluid under the same conditions) while

from TEM photomicrograph the mean D_P (equivalent diameter corresponding to the diameter of a sphere with the same projected area as the particle) is derived [4, 5].
From this investigation it can be stated that the use of a single approach to estimate NP size has some limitation. In addition, the use of the sole image analysis of TEM photomicrograph, often reported in literature [6, 7], may lead to underestimation of the existing particle population. A last consideration will concern the image quality for elaboration that can hinder particle recognition.

References

[1] Xie J et al, Adv. Drug Deliv. Rev. 62, 1064 (2010);
[2] Boisselier E et al, Chem. Soc. Rev. 38, 1759 (2009);
[3] Dreaden EC et al, Chem. Soc. Rev. 41, 2740 (2012);
[4] Pabst W et al, ICT Prague (2007);
[5] Barber TA, Pharmaceutical particulate matter-analysis and control. Interpharm press (1993);
[6] Daniel MC et al, Chem. Rev., 104, 293 (2004), Vol. 104;
[7] Sakai T et al, Langmuir, 20, 8426 (2004).

EFFECT OF MICELLES FORMATION AND DRUG LOADING ON THERMAL PROPERTIES OF INULIN-GRAFT-VITAMIN E (INVITE) POLYMERS

GIUSEPPE TRIPODO[1], LAURA CATENACCI[1], DELIA MANDRACCHIA[2], MILENA SORRENTI[1]

[1]Department of Drug Sciences, University of Pavia, Viale Taramelli 12, 27100 Pavia, Italy
[2]Department of Pharmacy, University of Bari "Aldo Moro", Via Orabona 4, 70125 Bari, Italy

Introduction

Using nanosized drug delivery systems to overcome solubility issues of hydrophobic drugs became in the last years more and more important. In this field, amphiphilic polymers, showing solubility differences between hydrophilic and hydrophobic segments, are known to assemble in an aqueous environment into nanosized polymeric micelles.[1] Exploiting polymeric micelles for drug delivery requires that several important parameters such as micelle stability, drug loading capacity, critical aggregation concentration CAC or interaction with the loaded drug have to be carefully considered and optimized in each application.[2] Nanostructured self-assembling inulin-graft-α-tocopherol (INVITE) polymers and micelles have been prepared and characterized in terms of thermal behavior. The core components of this amphiphile system are Inulin (INU) and Vitamin E succinate (VITE). INU has been chosen for its unique features: i) it is totally filtered by kidney and it is not secreted or reabsorbed at any appreciable amount at the nephron; ii) it is highly biocompatible; iii) it is selectively degraded by colonic bacteria.[3] These features make INU an useful tool for drug delivery of drugs in different sites. On the other side VITE: i) decreases serum lipid peroxidation and improves renal function after kidney transplant; ii) preserves the integrity of biological membranes and prevents apoptosis due to oxidative stress; iii) promotes neutral endothelial vasoactivity, decreases the adhesion of monocytes to endothelium, and decreases the superoxide production by activated phagocytes and inhibits platelet aggregation; iv) shows a low toxicity even at high concentrations.[4]

Goal of the work

In order to verify the effect of different processes on the starting polymers INVITE, their thermal properties have been deeply investigated. In particular, micelles from INVITE polymers, at different degrees of substitution in VITE, have been prepared by the dialysis method so obtaining three different micelle systems. The same systems have been further loaded with the hydrophobic drug curcumin with the aim to evaluate the influence of a hydrophobic drug in the micelles core. These studies are aimed to verify whether the tested systems could result stable at physiological temperatures and how the different parameters tested such as lyophilization, micelle formation or drug loading might influence the overall thermal behaviors of the systems for an optimized preparation of the subsequent formulation.

Experimentals

Inulin-α tocopherol conjugates (INVITE) were synthesized at different degree of substitution in vitamin E succinate (VITE). Briefly, VITE was dissolved in DMF and DCC and NHSS were added. Then, Inulin (INU) and triethylamine (TEA) were added and the reaction, according to a molar rate VITE/INU 0.1, 0.2 or 0.4 was carried out under nitrogen at 25 °C for 24 h and the corresponding INVITE 1, INVITE 2 and INVITE 3 polymers, were recovered from acetone.
For drug loading, 100 mg of INVITE were solubilized in 10 ml of DMSO, then 3 mg of Curcumin were added. After complete solubilization, the solution was poured in a dialysis tube with a molecular weight cut off (MWCO) 3.500 Da and dialyzed against distilled water for 3 days. The clear/yellow solution has been lyophilized and recovered with 86 % w/w yield with respect to the starting polymer. The same method, without drug, was used to obtain the drug loaded or not INVITE micelles. Curcumin loaded micelles were solubilized in DMSO and drug loading was calculated by means of UV-VIS determination. For stability studies, the hydrodynamic size of the INVITE micelles and the polydispersity index, were measured by photon correlation spectroscopy using a Zetasizer Nano ZS (Malvern Instruments Ltd., Worcestershire, UK). In particular, the size of INVITE micelle in aqueous solutions was valued at 25 °C after pre-defined storage time up to 60 days to verify their physical stability.
Temperature values were measured with a Mettler STAR^e system (Mettler Toledo) equipped with a DSC821^e Module and an Intracooler device for subambient temperature analysis on 2–3 mg samples in sealed aluminum pans with pierced lid. DSC curves were performed over a temperature range of 30-250 °C for INU and VITE (β =10 K min^{-1}, nitrogen air atmosphere flux (50 ml min^{-1})). To better characterize the INVITE conjugates the samples were heated to 160 °C then cooled to -20 °C and heated again to 160 °C (β =30 K min^{-1}, nitrogen air atmosphere flux (50 ml min^{-1})). The midpoint of the deflection in the heat flow

versus temperature curve, referred to the second heating cycle, was taken as the T*g*.
Mass losses were recorded with a Mettler STAR^{e} system TG simultaneously DSC (TG/DSC1) on 3-4 mg samples in open alumina crucibles (β =10 K min^{-1}, nitrogen air atmosphere (flux 60 ml min^{-1}), 30–400 °C temperature range).
The instruments were preventively calibrated with Indium as standard reference. Measurements were carried out at least in triplicate.

Results and discussion

INVITE polymers have been synthesized at different degree of substitution in VITE. This lead to amphiphilic systems able to solubilize the hydrophobic drug curcumin. Micelles from INVITE polymers have been obtained by the dialysis method. After freeze drying of the dialyzed micelles a white, soft and easy redispersible solid has been obtained. The same micelles have been prepared in the presence of curcumin as a model of hydrophobic drug with water solubility as low as 11 ng/ml. Also in this case, the displacement of DMSO during the dialysis to obtain the INVITE drug loaded micelles resulted in a transparent and, in this case, yellow solution, so indicating that the drug was totally incorporated into the micelles core. The freeze dried drug-loaded micelles resulted in a yellow, soft and easy redispersible solid.
The native polymers, empty micelles and drug-loaded micelles were characterized by thermal methods (DSC and TG analysis). The results indicated that all tested samples have a T*g* value higher than 60 °C indicating that micelles, empty or drug-loaded, could result stable at 37 °C so being their stability at least not affected by the temperature. Also TG analysis– confirmed this trend; the decomposition was in all cases recorded over 160 °C. In particular, a trend in thermal stability has been seen in the order INVITE 1 < INVITE 2 < INVITE 3. The presence of the drug seems to better stabilize the micelles.
The isothermal stability of drug loaded or not micelles has been also valued by determining the micelle size at different time points until 60 days. The investigated systems did not show any particular instability in terms of micelles size even if this aspect is still under investigation.

Conclusion

These preliminary results show that INVITE polymers or micelles (drug loaded or not) are stable by a thermal point of view and not particular differences can be observed for drug loaded or not micelles.

References

[1] R. Zana, Langmuir, 12 (1996) 1208-1211.
[2] L. Di, P.V. Fish, T. Mano, Drug Discovery Today, 17 (2012) 486-495.
[3] M.B. Roberfroid, Journal of Nutrition, 137 (2007) 2493S-2502S.
[4] M.A. Thabet, J.C.M. Chan, Pediatric Nephrology, 21 (2006) 1790-1801.

FUNCTIONALITATION OF HYDROPHOBIC SURFACES WITH A POLYASPARTAMIDE-BASED DERIVATIVE FOR BIOMEDICAL APPLICATION

C. Sardo[1], B.Nottelet[3], D. Triolo[1], G. Giammona[1,2], X. Garric[3], JP-Lavigne[4], G. Cavallaro[1], J. Coudane[3]

[1]Laboratory of Biocompatible Polymers, Dipartimento di Scienze e Tecnologie Biologiche Chimiche e Farmaceutiche (STEBICEF), Università di Palermo, via Archirafi 32, 90123 Palermo, Italy.
[2] IBF-CNR, via Ugo La Malfa,153, 90146 Palermo, Italy.
[3]Institut des Biomolécules Max Mousseron UFR Pharmacie – Université Montpellier I, 15, Avenue Charles Flahaut 34093 Montpellier, France.
[4]Bacterial Virulence and Infectious Disease, INSERM U1047, University of Montpellier 1, UFR Médecine Site de Nîmes, 186 Chemin du Carreau de Lanes, CS 83021, 30908 Nîmes Cedex 2, France.

Introduction

A convenient way for the achievement of polymer-based solid materials for specific biomedical applications is grafting the appropriate macromolecules onto the surfaces in order to confer them specific properties. To date many approaches have been used to covalently modify polymeric surfaces, and among them chemoselective coupling reactions, usually referred as "click" reactions, gained much attention thanks to simple procedure with high reaction rate under mild reaction conditions (at normal temperature and pressure) [1]. In particular, radical-initiated thiol-yne "photo-click" chemistry has been demonstrated as an effective way to functionalize efficiently surfaces.

In this frame, copper catalysed "click" chemistry was recently used to confer antibacterial and antibiofilm properties to propargylated PLA surfaces by immobilization of polyquaternary ammoniums [2].

Goal of the work

PHEA is a highly water soluble synthetic polymer possessing important properties such as hydrophilicity, biocompatibility and non immunogenic activity, that allow to use it as a polymer for biomedical applications [3]. Moreover the large number of hydroxyl groups make PHEA a versatile platform for the derivatization with molecules of various molecular weight.

In this work a PHEA based copolymer bearing in the side chains ethylendiammine (EDA) and carboxypropyl trimethylammonium (CPTA) groups, PHEA-EDA-CPTA [4], has been modified with lipoic acid to obtain a polycation easily graftable on clickable propargylated PLA_{94} surfaces prepared according to a previously described procedure [5].

The rationale for these approaches was to use the biocompatibility and biodegradability of PHEA based copolymers and the well known properties of polycations to act as biocidal for a broad spectrum of pathogenic microorganisms [6] to design an implantable antibacterial PLA_{94} surface, which would prevent the initial attachment of bacteria, therefore preventing the subsequent formation of a biofilm.

Results and discussion

The polycationic copolymer PHEA-EDA-CPTA-LA was synthesized in very high yields (86 w%) starting from a PHEA-EDA-CPTA with a molar derivatization degree ($DD_{mol\%}$) of 50% in EDA, while the $DD_{mol\%}$ in CPTA was of 26.5%. To introduce in side chain a group suitable for thiol-alkyne photo-click coupling on propargylated PLA_{94} surface, lipoic acid was linked to PHEA-EDA-CPTA copolymer. Lipoic acid infact contains a dithiolane ring that after proper reduction is prone to react with triple bonds of propargylic groups. The reaction was conducted in very mild conditions performing a specific and practical carbodiimide-mediated conjugation between the carboxylic group of LA and free primary amino groups of EDA in PHEA-EDA-CPTA (Scheme 1). The new copolymer was characterized by ^{1}H NMR and a $DD_{mol\%}$ in LA equal to 13.5% was found.

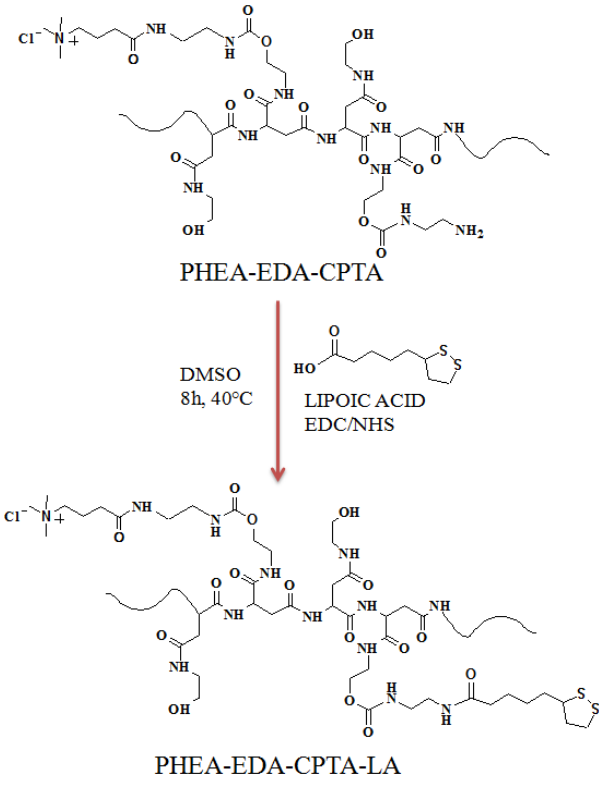

Scheme 1. Scheme of the synthesis of PHEA-EDA-CPTA copolymer.

A ‘‘clickable’’ PLA surface obtained via anionic activation, following a recently described method (Figure 1), was prepared and then functionalized with the obtained PHEA-EDA-CPTA-LA copolymer by a radical-initiated thiol-yne “photo-click” reaction, after proper reduction of disulfide bonds of LA portions using a water soluble phosphine. This approach of covalent immobilization on the surface gives the possibility to avoid the presence of residual metal impurities and to increase the density of surface functionalization, thanks to the possibility to yield bis-addition products on triple bonds [7].

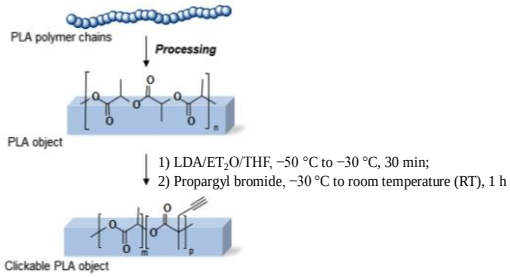

Figure 1. ‘‘Clickable’’ PLA surface obtained via anionic activation [2],[5].

As the chemical modification takes place only at the surface of the propargilated PLA_{94} object, XPS analysis was performed to show the presence of elemental constituents of PHEA-EDA-CPTA-LA on the modified surface.

To fully demonstrate the covalent immobilization, a fluorescent probe was bounded to PHEA-EDA-CPTA-LA free primary amine groups and refractometric and fluorometric SEC analyses of the PLA surface modified with the fluorescent polymer was performed.

The anti-adherence and antibiofilm activities of modified PLA surfaces was assessed. Antibacterial PLA surfaces showed to be very active against both Gram-negative and Gram-positive strains, with a surprisingly higher adherence reduction than on starting material and a marked reduction in biofilm formation (figure 2).

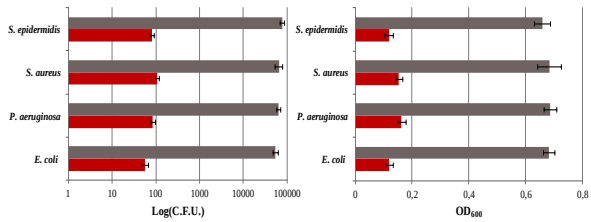

Figure 2. anti-adherence and antibiofilm activities of PHEA-EDA-CPTA-LA modified PLA_{94} surfaces. Gray bars represent PLA control.

Further, it was investigated on the biocompatibility of PHEA-EDA-CPTA-LA modified PLA_{94} surfaces monitoring *in vitro* the proliferation of mouse fibroblasts. In addition to the substantial antibacterial activity, the proposed PLA_{94} surfaces modified with the polycationic PHEA derivative resulted also cytocompatible.

Conclusion

Antibacterial PLA surfaces were prepared by the ‘‘grafting onto’’ technique using a polycationic PHEA derivative, PHEA-EDA-CPTA-LA. This was achieved by combining mild anionic activation of the PLA surface, ensuring no degradation of the polyester, with a highly efficient thiol-yne photo-click grafting under mild heterogeneous conditions.
The obtained surfaces were highly efficient against the bacterial strains tested, including Gram-negative and Gram-positive bacteria, by decreasing their adherence and biofilm formation. Moreover, the new antibacterial surfaces were found to be cytocompatible and should be considered for future investigations in the field of implantable degradable biomaterials.

References

[1] Casey J. Galvin, Jan Genzer; Progress in Polymer Science 2012;37:871-906.
[2] S. El Habnouni, J-P. Lavigne, V. Darcos, B. Porsio, X. Garric, J. Coudane, B. Nottelet. Acta Biomaterialia 2013;9:7709-7718.
[3] Mendichi R, Giammona G, Cavallaro G, Giacometti Schieroni A. Polymer 2000;4:8649–57.
[4] Licciardi M, Campisi M, Cavallaro G, Cervello M, Azzolina A, Giammona G. Biomaterials 2006;27:2066-2075.
[5] S. El Habnouni, V. Darcos, X. Garric, J-P. Lavigne, B. Nottelet, J. Coudane. Advanced functional Materials 2011;21(17):3321-3330.
[6] Hasan J, Crawford R J, Ivanova E P. Trends in Biotechnology;2013;31(5): 295-304.
[7] Cang Wang, Yan Fan, Meng-Xin Hu, Wei Xua, Jian Wua, Peng-Fei Ren, Zhi-Kang Xu; Colloids and Surfaces B: Biointerfaces 2013;110:105-112.

IMPLANTABLE NANOCHANNEL DELIVERY SYSTEM FOR THE SUSTAINED RELEASE OF ULTRA-STABLE LIPOSOMES

Christian Celia[1,a,b,*], Silvia Ferrati[1,b], Shyam Bansal[b], Anne L. van de Ven[b], Barbara Ruozi[c], Erika Zabre[b], Sharath Hosali[d], Donatella Paolino[e], Maria Grazia Sarpietro[f], Daniel Fine[b], Luisa Di Marzio[a], Martina Di Francesco[a], Massimo Fresta[e], Mauro Ferrari[b,g,h,i], and Alessandro Grattoni[b].

aDepartment of Pharmacy, University of Chieti – Pescara "G. d'Annunzio", Via dei Vestini 31, Chieti 66013, Italy.
bDepartment of Nanomedicine, The Methodist Hospital Research Institute, 6670 Bertner Ave. Houston, TX 77030, USA.
cDepartment of Life Sciences, University of Modena and Reggio Emilia, Via Campi 183, Modena
dNanoMedical Systems, Inc., 2706 Montopolis Drive, Austin, TX 78741, USA.
eDepartment of Health Sciences, University of Catanzaro "Magna Graecia", V.le "S. Venuta" Germaneto-Catanzaro 88100, Italy.
fDepartment of Drug Sciences, University of Catania, V.le A. Doria 6, Catania 95125, Italy.
gDepartment of Medicine, Weill Cornell Medical College, 1300 York Avenue, New York, NY 1006, USA.
hDepartment of Bioengineering, Rice University, 6100 Main Street, Houston, TX 77251, USA.
iAlliance for NanoHealth, 6670 Bertner Ave., Houston, TX 77030, USA.

Metronomic chemotherapy supports the idea that long-term, sustained, constant administration of chemotherapeutics, currently not achievable, could be effective against numerous cancers. Particularly appealing are liposomal formulations, used to solubilize hydrophobic therapeutics and minimize side effects, while extending drug circulation time and enabling passive targeting. As liposome alone cannot survive in circulation beyond 48 h, sustaining their constant plasma level for many days is a challenge. To address this, we develop, as a proof of concept, an implantable nanochannel delivery system and ultra-stable PEGylated lapatinib-loaded liposomes, and we demonstrate the release of intact vesicles for over 18 d. Further, we investigate intravasation kinetics of subcutaneously delivered liposomes and verify their biological activity post nanochannel release on BT474 breast cancer cells. The key innovation of this work is the combination of two nanotechnologies to exploit the synergistic effect of liposomes, demonstrated as passive-targeting vectors and nanofluidics to maintain therapeutic constant plasma levels. In principle, this approach could maximize effi cacy of metronomic treatments.

"DOUBLE-DECKER" SCAFFOLDS MADE OF SILK FIBROIN

F. Cilurzo, F. Selmin, C.G.M. Gennari, P. Minghetti, L.Montanari

Università degli Studi di Milano, Dipartimento di Scienze Farmaceutiche – via G. Colombo, 71 Milano

Silk fibroin (SF) of the Bombyx mori silkworm has been widely studied in tissue engineering due to the combination of mechanical strength with versatility in processing and biocompatibility.
Electrospinning, freeze drying and salt leaching are commonly used techniques to form 3D-scaffolds. Microarchitecture and fiber orientation within scaffolds can have significant effects on various cell behaviors including cell migration, orientation, adhesion and proliferation dictating cellular function and influencing tissue growth [1,2]. Afterwards, a final curing manipulating the secondary structure of fibroin (i.e. the ratio between the β-sheets and random-coil regions) is required to improve its water stability and enhance mechanical properties of the scaffold. To accomplish this goal, processes based on the use of organic solvents [5], water-based annealing [6] or water vapour [7] at room temperature have been proposed.

The present work reports the impact of freeze drying method on the architecture and mechanical properties of SF scaffolds aiming to obtain a sponge- or oriented lamellar-like structure by a solvent free process.

The degummed Bombyx mori fibers were completely dissolved in the Ajisawa reagent and dialyzed for 3 days. The solution concentration calculated on the basis of the dried weight, was 3% w/w. Scaffolds were prepared by freeze dried 3 mL SF solution in glass vials. Two different cooling procedures were applied in the freezing step: in the former samples were frozen at -20 °C for at least 8h (cooling strategy A); in the latter, after ice nucleation the sample was thawed at -10 °C to favor the crystal growth for 1h (cooling strategy B) or 2h (cooling strategy C); then, the freezing was carried out according to the "Cooling strategy A".
Afterwards, scaffold were sterilized by vapour steam sterilization.
The morphology of scaffolds was analyzed by SEM and microTC. The open porosity (π) was calculated by a solvent displacement method. Molecular conformation of SF was determined by ATR-FTIR spectroscopy.
Scaffolds were incubated in 30 mL of pH 7.4 PBS in a horizontal shaker incubator at 37±1 °C and at predetermined time points (i.e. 1, 7, 14 and 28 days), mechanical properties were determined by means of cyclic compression test. The following parameters were calculated from the strain stress-curve: resistance to compression (σ); compressive modulus (E_c) calculated as the slop of the linear portion of the first loading step; total range strain (Δε) calculated as the difference between the ε_{66} and ε_{min} of each cycle; hysteresis loop (W) calculated as the difference between the loading and unloading works of each cycle; secant modulus (Es) determined according to the following relationship: $Es = \sigma_{66}/ \Delta\varepsilon$.

Both cooling strategy resulted in SF solutions supercooled at –8 °C prior to spontaneous ice nucleation (**Figure 1**). The thawing step in the Cooling strategies B and C permitted to maintain SF solution at the nucleation temperature for about 1 and 2 additional hours, respectively (**Figure 1**).

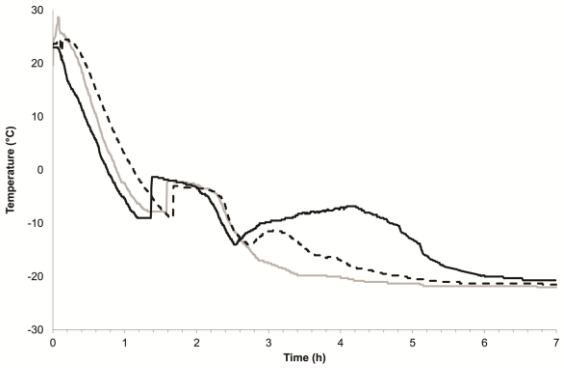

Figure 1. Typical plot of a SF solution frozen according to the different cooling strategies. Cooling strategy A (grey, solid line), Cooling strategy B (black, dash line) and Cooling strategy C (black, solid line).

In samples nucleating and freezing via the global supercooling mechanism (i.e. the entire liquid volume achieves a similar level of supercooling), the secondary nucleation zone encompasses the entire liquid volume [8]. As a consequence, the spherulitic morphology in the corresponding scaffold type A was probably due to the formation of spheroidal ice crystals concentrated the amorphous phase into a sponge-like matrix.

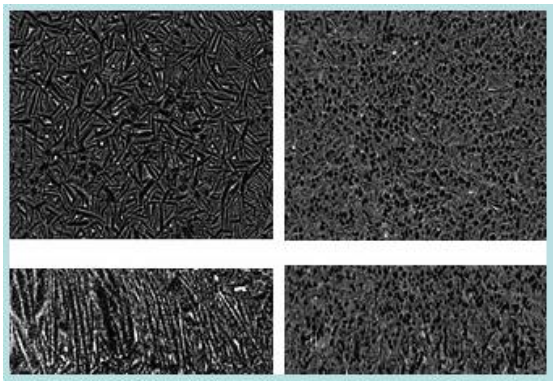

Figure 2. MicroTC images of scaffolds produced according to the cooling strategy B.

Two layers at different morphologies were evident in scaffolds prepared following the cooling strategy B

(**Figure 2**). In the left panel, the upper part presents an oriented stacked leaf-like structure oriented toward the center of the matrix. In addition, the lamellae have a solid surface with interconnected voids among them such that a porous structure is present. This morphology was also evident in scaffolds obtained by cooling strategy C. The right panel shows a sponge-like matrix typical of scaffolds obtained by cooling strategy A (**Figure 2**).

Scaffolds presented a good interconnectivity with a pore dimension of about 50 µm, independently of the cooling strategy. Differences in morphology determined differences in porosity which increased from 85% to about 94% shifting from a sponge-like structure towards the leaf-like structure. After sterilization, both porosity and interconnection were well-preserved, even if a 4-5% reduction was determined.

Spectral deconvolution of amide I region of the relative ATR-FTIR spectra was used to quantify protein secondary structure content for each processing condition [9].

The contributions of peak areas attributed to different components evidenced a prevalence of the Silk I conformation independently of the cooling strategy. The thawing step lead to a higher amount of β-sheet fraction in the lamellar-like (~28.5%) structure with respect to the sponge-like portion (~34%). Steam sterilization induced a modification in the fibroin secondary structure content, causing an increase in the β-sheets content along with a decrease in α-helix/random coil content and nullifying the differences in β-sheets content.

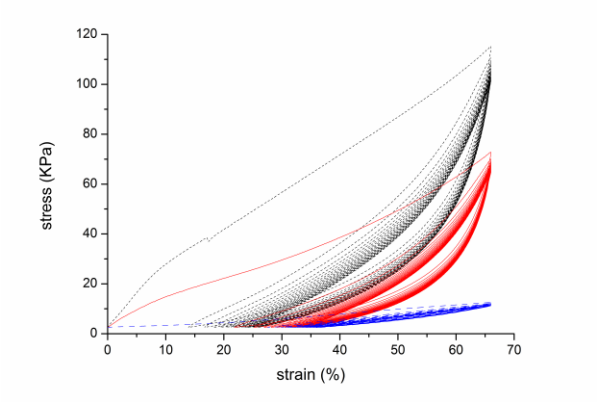

Figure 3. Cyclic compression of scaffolds of sponge-like scaffolds (black line) and "double-decker" scaffolds (red line) and lamellar like-scaffolds (blue line) incubated for 1 day in PBS at 37 °C.

The stress-strain curves of the scaffolds incubated for 1 day evidenced that the mechanical properties were modified by the scaffold inner morphologies (**Figure 3**). In particular, the linear region in the first loading step was recorded until 8% of the ε value was reached. Afterwards, the compression behavior of the scaffold changed probably because of a concomitant densification of structure due to porous deformation and extrusion of water outside the scaffold. During the unloading step, the scaffold inner organization returned to the original one re-absorbing the squeezed out water. Therefore, the energy related to the elastic deformation and resistance due to the presence of water was partially dissipated. Moreover, the first hysteresis loop, which is a measure of dissipated energy, appeared significantly higher with respect to those of the following cycle.

The variation of σ_{66} and $\Delta\varepsilon_t$ as function of the loading and unloading cycle decreased following a semi-logarithmic pattern ($r^2 > 0.9982$).

As the reduction of the resistance to compression was concomitant of the decrease of the hysteresis area calculated over the first cycle, this feature can be considered as an indication of the ability scaffold to recover its initial structure after removing the load.

The slight gradual increase of the secant modulus with the number of cycles was taken as a confirmation of the progressive compaction of fibroin chains and partial rearrangement of the microstructure during repeated compressive loading. This means that scaffolds were substantially able to rearrange the inner structure in order to support the stresses over loading–unloading cycles without undergoing to significant permanent changes.

The trend described for sponge-like scaffolds fit also the behavior of "double-decker" scaffolds, despite the significant increase in the σ_{66} values. These differences were attributed to the orientation of the lamellae toward the z-axis, which increased the resistance to compression of the structures. Surprisingly, the scaffold obtained prolonging the thawing step exhibited the lowest σ_{66} because of a different pattern of the scaffold during the loading step, which was performed in unconstrained condition.

In conclusion, the inner architecture of SF scaffolds, obtained by a solvent free process, can be tuned by the introduction of a thawing step during the freeze-drying process. The shifting from a sponge-like to a lamellar-like structure played a significant effect on porosity and mechanical properties of such scaffold. Both these properties can be potentially modulated by the length in time of the thawing step, which controls the ratio between the two types of morphology. Thus, "double-decker" scaffolds could be advantageously produced when the differentiation of the cell lines requires different porosity or an increase of the stiffness of the structure along a single direction.

References:

[1] Agarwal S et al., Polymer 49, 5603 (2008).
[2] Funatsu K et al., Artif Organs 25, 194 (2001).
[3] Zhang Q et al., Acta Biomaterialia 8(7), 2628 (2012).
[4] Oliveira AL et al., Acta Biomaterialia 8, 1530 (2012)
[5] Nazarov R et al., Biomacromol 5, 718 (2004).
[6] Jin HJ et al., Adv Funct Mater 15, 1241 (2005).
[7] Min BM et al., Macromol Biosci 6, 285 (2006).
[8] Searles et al., J Pharm Sci 90(7), 860 (2001).
[9] Cilurzo et al., Int J Pharm 414, 218 (2011).

MICROSCOPY CHARACTERIZATION OF MICRO- AND NANO-SYSTEMS FOR PHARMACEUTICAL USE

R. CORTESI[1], M. DRECHSLER[2], E. ESPOSITO[1]

[1]Department of Life Sciences and Biotechnology, University of Ferrara, Ferrara, Italy
[2] Electron microscopy Macromolecular Chemistry II, University of Bayreuth, Bayreuth, Germany

Introduction

In pharmaceutical field the use of microscopy has been exerted an important role since the advent of micro and nanotechnology. Indeed the morphology of particles and their inner structure does influence the modalities of administration and release of encapsulated drugs.
Scanning electron microscopy (SEM) can be employed to study the morphology of dry powders, in particular microparticles made of polymers can be well visualized and their diameters can be measured. By cutting the powder during sample preparation, it is possible to obtain important information about the inner morphology of the microstructures, discriminating either the capsule or the sphere microstructure.
Cryo transmission electron microscopy (cryo-TEM) is a precious tool for characterizing colloidal systems. In particular external as well as internal shape of nanoparticulate systems such as solid lipid nanoparticles or lyotropic mesophases can be well identified. Moreover size of disperse phase and the overall structure of the dispersion can be monitored.

Goal of the work

The purpose of this research project is a focus on the use of electron microscopy as technique for characterizing microparticles and nanosystems recently developed by our research group. In particular polyesters microparticles, solid lipid nanoparticles (SLN), nanostructured lipid carriers (NLC) and monooleine aqueous dispersion (MAD) are presented.

Experimentals

Production of microparticles and nanoparticles
Microparticles were produced by the 'solvent evaporation method' [1]. SLN and NLC were prepared by stirring followed by ultrasonication [2]. MAD were alternatively produced by the hydrotrope or by the hot homogenization methods [3,4].

Scanning and Cryo-Transmission electron microscopy analyses
For SEM analysis microparticles were metallized by gold coating (Edwards Sputter coat-ing S150) and visualized at 15 – 20 kV with a 360 Stereoscan (Cambridge Instruments, Cambridge, UK).
For Cryo-TEM analysis samples were vitrified and transferred to a Zeiss EM922Omega (Zeiss SMT, Oberkochen, Germany). Images were recorded by a CCD digital camera (Ultrascan 1000, Gatan) and analyzed using a GMS 1.8 software (Gatan).

Results and discussion

The morphology of microsystems can influence the release of the encapsulated drug. SEM enables to discriminate the surface aspect of microspheres focusing on the presence or the absence of pores, indeed the porosity is a factor that can promote drug release. Moreover, the obtaining of cross-sectioned microparticles enables to observe the inner structure. Drug release from the microparticles can be understood by considering the geometry of the carrier. Depending on the type of polymer and on the method of production, different type of microparticles can be achieved.
Figure 1 reports images showing external and internal morphology of empty DL-PLGA 50:50 microparticles produced by the solvent evaporation method, using as solvent methylene chloride (panels A and B) or ethyl acetate (panels C and D). It is interesting to note that methylene chloride induces the formation of irregular shaped microparticles with different dimensions, whereas the use of ethyl acetate results in round microparticles with smooth surface and homogeneous dimensions. Moreover, analyzing the cross section, it can be noted that the use of methylene chloride allows the production of mononucleate microcapsules with a classic reservoir structure, while the particles by ethyl acetate show a multinucleate structure. This result can be attributed to the different evaporation rates of the solvents, in fact methylene chloride (boiling point 40°C) evaporates more rapidly than ethyl acetate (boiling point 77 °C).
In the case of nanosized liquid systems, cryo-TEM is an optimal method to obtain structural information, revealing morphology and inner details of the samples studied. Figure 2 shows cryo-TEM images of SLN and NLC dispersions. In particular panel A shows an image of plain SLN, panel B refers to plain NLC, while panels C and D respectively show prednisone and bromocriptine containing NLC.
The three dimensional particles are projected in a two dimensional way. In all panels, depending on the angle of observation in the vitrified samples, the particles appear as deformed hexagonal, elongated circular platelet-like crystalline (SLN/NLC top views) or "needle" like structures edge-on viewed (SLN NLC side views).
The measured thickness of nanoparticles is between ca. 5 nm and 40 nm, according to the number of layers in the platelets.

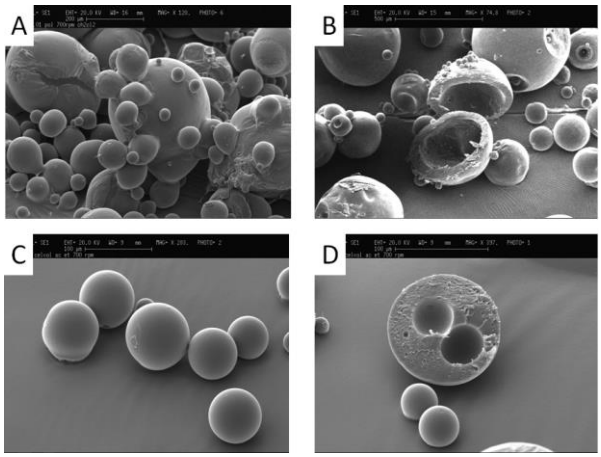

Fig. 1. SEM images of DL-PLGA 50:50 microparticles produced by the solvent evaporation method, using as solvent methylene chloride (A,B) or ethyl acetate (C, D)

However the exact thickness is difficult to measure since the tilt of the particles can't exactly be determined. In panels B, C and D, besides the presence of hexagonal and circular NLC top views, the "needles" are more elliptically shaped, with respect to the SLN side views (panel A). This may be attributed to the presence of Miglyol 812 forming compartments adherent to the surfaces of the nanoparticles' solid matrix. This behavior is clearly noticeable in the presence of prednisone and bromocriptine (panels C and D).

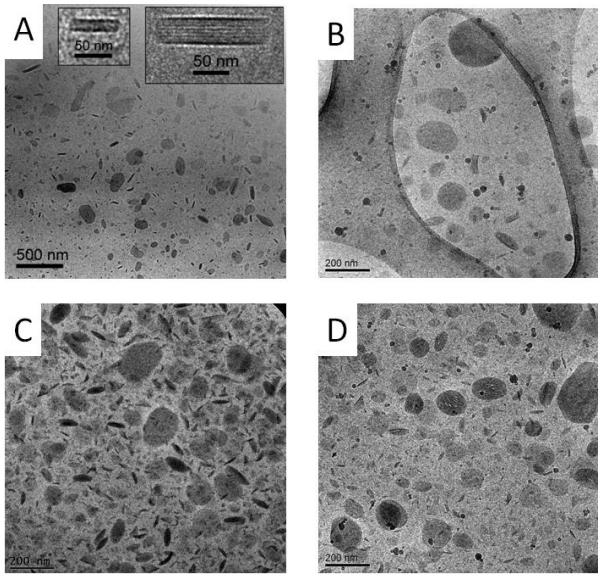

Fig 2. Cryo-TEM images of empty SLN (A), empty NLC (B), prednisone containing NLC (C) and bromocriptine containing NLC (D).

Figure 3 shows two aqueous dispersions of monooleine produced in the presence of Poloxamer 407 obtained by the hydrotrope (Panel A) or by the hot omogenization method (Panel B). Some authors have reported that the method resulted in the production of cubosome dispersions. Nonetheless in this case only differently shaped vesicular structures mainly unilamellar or with some invaginations were obtained.

Whereas the dispersion reported in panel B displays the coexistence of vesicles and spherical particles with a homogeneous ordered inner structure typical of cubosome.

The presence of vesicular structures attached on the surface of cubosomes suggests that through time, a transformation may take place from conglomerates of partially fused vesicles to well-ordered particles. Considering a number of pictures taken from cryo-TEM observation, dimensions can be measured finding that two different populations are often present: one constituted of large cubosomes (size over 200 nm) and another of smaller cubosomes and vesicles with sizes about 100 nm and below.

Fast Fourier transform (FFT) easily enables to obtain an optical diffractogram similar to an electron diffraction pattern. FFT is therefore a precious mean to identify the different type of liquid crystalline structures. In Fig. 3B patterns with rectangular symmetry with differently sized 2D lattice parameters are present. In particular lattice cubic particles with parameters of 7.1 x 10.2 nm (labeled a) and 7.1 x 8.9 nm (labeled b) can be observed. Moreover also the diagonal dimension can be measured (labeled c).

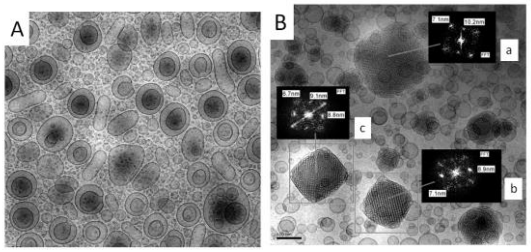

Fig. 3 Cryo-TEM images of MAD obtained by the hydrotrope (A) and the hot homogenization (B) methods. The insets show the FFT lattice parameters of the indicated nanostructures.

Conclusion

Microscopy is to be considered as an indispensable tool to study drug delivery systems.

In particular SEM is helpful in giving information about micro-sized powders, allowing to identify microspheres and microcapsules, as well as to obtain size distribution of the observed particles.

Colloidal drug delivery systems, filling the most part of pharmaceutical panorama in nanotechnology field, can be unambiguously detected by the use of cryo-TEM. Charming images can reveal the external and inner structure of nanosystems, giving information about the drug release modality of the included molecules and suggesting their suitability for the chosen type of administration.

References

[1] P.B. O'Donnell et al, Adv. Drug. Del. Rev. 28 (25) (1997).
[2] E. Esposito et al, Pharm. Res. 25 (1521) (2008).
[3] P.T. Spicer et al, Langmuir 17 (5748) (2001).
[4] E. Esposito et al, Pharm. Res. 22 (2163) (2005).

ENHANCED BRAIN TARGETING OF ENGINEERED SOLID LIPID NANOPARTICLES

R. Dal Magro[1], F. Ornaghi[1], I. Cambianica[1], S. Beretta[1], F. Re[1], A. Brambilla[1], F. Barbero[2], C. Musicanti[2], A. Cagnotto[3], E. Donzelli[4], A. Canta[4], M. Masserini[1], G. Cavaletti[4], P. Gasco[2], G. Sancini[1]

[1] Department of Health Sciences, University of Milano-Bicocca, via Cadore 48, 20900 Monza, MB, Italy.
[2] Nanovector S.r.l., via Livorno, 60 - 10144 Torino, TO, Italy.
[3] Department of Molecular Biochemistry and Pharmacology, Mario Negri Institute for Pharmacological Research, via La Masa 19, 20156 Milano, MI, Italy.
[4] Department of Surgery and Translational Medicine, University of Milano-Bicocca, via Cadore 48, 20900 Monza, MB, Italy.

The blood-brain barrier (BBB) plays an important role in maintaining the homeostasis of the central nervous system and in protecting the brain from potentially harmful endogenous and exogenous compounds. Nevertheless it represents also the major obstacle for the diagnosis and therapy of brain diseases. One of the most promising strategies to overcome the limited BBB penetration of drugs and contrast agents is based on nanoparticles (NP). Lipid based NP, basically liposomes and solid lipid nanoparticles (SLN), have several advantages in terms of biocompatibility, non-immunogenicity, non-toxicity; they can be used as carrier systems [1], and they have a high blood circulation residence time [2]. Moreover their surface can be easily modified with ligands which mediate a site-specific targeting.

Here we evaluated the ability to cross the BBB and reach the brain district of SLN, radiolabelled or loaded with different fluorescent dyes, covalently coupled by DSPE-PEG(2000)-Maleimide with the monomer of ApoE-residues (141-150) [3] and functionalized with phosphatidic acid (Aβ ligands) [4]. SLN cell uptake was monitored by confocal-laser-scanning microscopy and quantified by radiochemical techniques [5]. The ApoE monomer mediated an efficient cellular uptake of SLN within cultured human cerebral microvascular endothelial cells (hCMEC/D3). SLN without surface-located peptide displayed less membrane accumulation and cellular uptake. In order to assess the ability of ApoE monomer to enhance SLN transcellular transport we employed an in vitro BBB model, based on hCMEC/D3. With respect to the un-functionalized SLN, the presence of monomer ApoE significantly enhanced their permeability through the cell monolayer (PE = $0.6 \cdot 10^{-5}$ cm/min vs PE = $6.95 \cdot 10^{-5}$ cm/min, respectively; Student's t-test, p value<0.05).

The biodistribution of SLN, loaded with DiR (fluoroprobe strictly associated to SLN), was evaluated by means of in vivo Fluorescent Microscopy Tomography (FMT 1500, Perkin Elmer). Our results confirmed the role of monomer ApoE in sustaining the delivery of SLN to the central nervous system, and allowed us to identify the intratracheal administration route (IT) as promising to enhance SLN biodistribution within the brain. Taken together these results suggest that the SLN formulation herein analyzed is a suitable tool for sustaining drug delivery to the brain.

References:

1. Priano L et al, Eur J Pharm Biopharm 79 (2011)
2. Gasco MR et al, Prog Brain Res 180 (2009)
3. Re F et al, Nanomedicine 7 (2011)
4. Gobbi M et al, Biomaterials 31 (2010)
5. Re F et al, J Biotechnol 156 (2010)

In Vitro and *In Vivo* Evaluation of an Oral Insulin Colon Delivery System

M.D. Del Curto[1], S. Salmaso[2], A. Maroni[1], F. Casati[1], P. Caliceti[2], A. Gazzaniga[1]

[1]Università degli Studi di Milano, Dipartimento di Scienze Farmaceutiche, Sezione di Tecnologia e Legislazione Farmaceutiche "Maria Edvige Sangalli", 20133 Milan, Italy.
[2]Università degli Studi di Padova, Dipartimento di Scienze Farmaceutiche, 35131 Padova.

Introduction

Oral colon delivery is currently explored as a strategy to improve the oral bioavailability of peptide and protein drugs [1,2]. Although the large bowel fails to be ideally suited for absorption, it may offer a number of advantages over the small intestine, including a long transit time, lower levels of proteases and a higher responsiveness to permeation enhancers. A time-dependent delivery system (Chronotopic™) based on a low-viscosity hydroxypropyl methylcellulose (HPMC) coating, which was demonstrated to provide the desired *in vitro* and *in vivo* release behaviour when conveying small molecules, was accordingly proposed for colonic release of insulin and selected adjuvants, such as protease inhibitors and absorption enhancers [3-6]. More recently, the design of the Chronotopic™ device, originally presented in single-unit configurations, was adapted to comply with the size requirements of multiple-unit dosage forms in view of their well-known benefits [7]. In particular, an insoluble, flexible film composed of the neutral polymethacrylate Eudragit®NE and the superdisintegrant sodium starch glycolate, added to act as a pore former, was applied to HPMC-coated minitablet cores in order to improve the efficiency of the hydrophilic layer in delaying the drug liberation without altering the typical release performance. The resulting two-layer formulation, containing acetaminophen as an analytical tracer, was shown to give rise to a prompt *in vitro* release after a lag phase of programmable duration and to the pursued *in vivo* behaviour [8]. Moreover, it was proved physically stable while stored under ambient conditions for 3.5 years.

Goal of the work

The aim of the present work was to prepare and evaluate *in vitro* as well as *in vivo* the above-described two-layer multiple-unit system as a possible colon delivery platform for insulin and the permeation enhancer sodium glycocholate.

Experimentals

Materials: bovine insulin and streptozotocin (Sigma-Aldrich, US-MO); copovidone (Kollidon®VA64, BASF, D); HPMC (Methocel®E50, Colorcon, I); hydroxypropyl methylcellulose acetate succinate (HPMCAS, Aqoat®AS-LG, Shin-Etsu, J, a gift from Seppic Italia, I); magnesium stearate (Carlo Erba Reagenti, I); microcrystalline cellulose (Avicel®PH200, FMC Europe, B); poly(ethylacrylate, methylmethacrylate) aqueous dispersion (Eudragit®NE30D, Evonik Röhm, D, a gift from Rofarma, I); polyethylene glycol (PEG 400, ACEF, I); sodium glycocholate (NaGly, Sigma-Aldrich, US-MO); sodium starch glycolate (Explotab® and Explotab®V17, Mendell, UK); male Sprague Dowley rats weighing 180-200 g fed ad libitum and handled in accordance with the provisions of the European Economic Community Council Directive 86/209 (recognised and adopted by the Italian Government with the approval decree D.M. No. 230/95-B) and the NIH publication No. 85-23, revised in 1985.

Preparation and in vitro release test: biconvex minitablets (2.5 mm) containing bovine insulin (0.4 mg) and NaGly (1:10), checked for weight, height, breaking force, friability and disintegration time, were coated with an 8% HPMC–0.8% PEG 400 aqueous solution (250 µm) by rotary fluid bed (GPCG1.1, Glatt, D) [9]. HPMC-coated cores were in turn coated by bottom-spray fluid bed with Eudragit®NE30D containing 20% w/w (on dry polymer) of Explotab®V17 (20 µm). Curing was then carried out at 40°C for 24 h. The two-layer system was finally coated with a 6.0% HPMCAS hydroalcoholic (ethanol 75% w/w) solution in a ventilated coating pan (GS, I). The enteric coating level was 7.5 mg/cm^2. *In vitro* release tests (n=3) were performed by a modified USP 35 disintegration apparatus (DT3, Sotax, CH, 37±1°C, phosphate buffer pH 6.8, 31 cycles/min, 160 ml) [10]. Gastroresistant systems were first tested in HCl 0.1 M for 2 h. Insulin and NaGly were assayed by RP-HPLC in fluid samples withdrawn at successive time points [5]. *In vitro* lag time was expressed as the time from pH change to 10% drug release ($t_{10\%}$). The test was repeated after three-month storage in glass vials at 4°C.

In vivo evaluation*:* Sprague Dowley male rats were subcutaneously treated with 65 mg/kg of streptozotocin. Animals with glucose levels of 400-500 mg/dl were divided into groups and administered orally with insulin-loaded coated and uncoated tablets or equal insulin amount in solution. At scheduled times, 50 µl of blood were collected by the tail vein and centrifuged. Plasma samples (10 µl) were diluted and the glucose concentrations were estimated with the Trinder Kit (Sigma). Plasma samples (10 µl) were used for insulin analysis as determined by ELISA using a human insulin-specific ELISA kit (Linco Research Inc., St. Charles, MO).

Results and discussion

In order to adapt the multiple-unit pulsatile delivery system under examination to a colon delivery platform, an outermost enteric film based on HPMCAS was applied so that the variability in gastric emptying time could be overcome. When evaluated for release, the

gastroresistant system showed no drug liberation during the acid stage of the test, which confirmed the formation of a continuous enteric film. On exposure of the system to simulated intestinal pH conditions, a pulsatile release of insulin and NaGly was observed after lag phases of reproducible and comparable duration (Fig. 1). The possibility of a concomitant liberation of the protein and the absorption enhancer was thus assessed. In addition, $t_{10\%}$ remained practically unchanged for both insulin and NaGly after 3 months of storage at 4°C, and no major differences were noticed in the release patterns (data not shown).

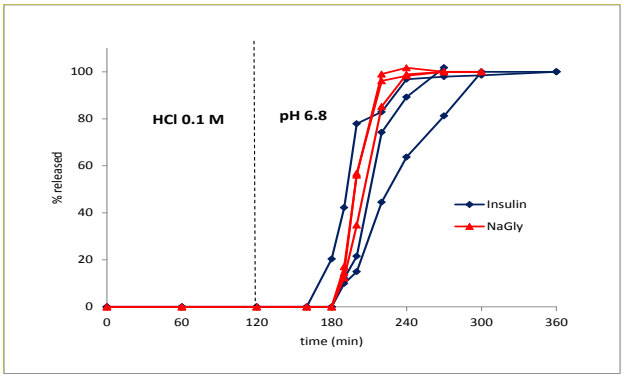

Fig. 1. Individual release profiles of insulin and NaGly from colon delivery systems.

As compared with an uncoated tablet formulation, the delivery system brought about a steep and significant rise in the plasma insulin concentration of diabetic rats, with a delayed peak after approximately 6 h from administration, and a corresponding decrease in the blood glucose levels (Fig.s 2 and 3).

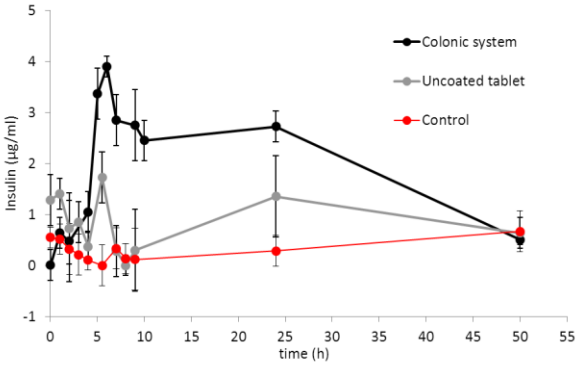

Fig. 2. Mean insulin plasma concentration vs. time profiles in untreated rats and following administration of either colon delivery systems or uncoated minitablets.

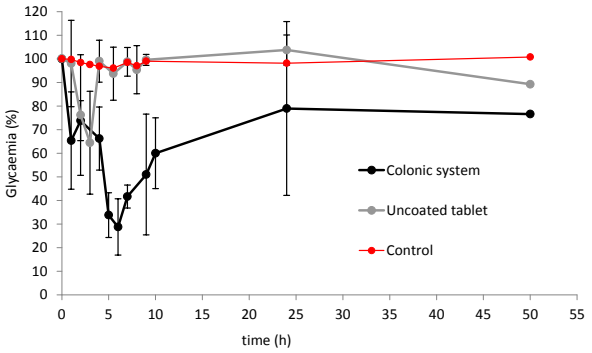

Fig. 3. Mean blood glucose concentration vs. time profiles in untreated rats and following administration of either colon delivery systems or uncoated minitablets.

Such results indicate that an effective and fast absorption of the hormone occurred from the gastrointestinal tract. Based on rat transit data from the literature, it can be assumed that the maximum insulin and minimum glucose concentrations would coincide with an ileo-colonic location of the delivery system [11,12].

Conclusion

The feasibility of a previously described two-layer multiple-unit delivery system for time-dependent colon release as an insulin carrier was demonstrated. The proposed system showed the desired *in vitro* and *in vivo* performance as well as the pursued hypoglycaemic effect.

References

[1] A Gazzaniga et al, Expert Opin Drug Deliv 3, 583-597 (2006).
[2] A Maroni et al, Adv Drug Deliv Rev 64, 540-556 (2012).
[3] ME Sangalli et al, J Control Release 73, 103-110 (2001).
[4] A Maroni et al, Eur J Pharm Biopharm 72, 246-251 (2009).
[5] MD Del Curto et al, J Pharm Sci 98, 4661-4669 (2009).
[6] MD Del Curto et al, J Pharm Sci 100, 3251-3259 (2011).
[7] A Maroni et al, Int J Pharm 440, 256-263 (2013).
[8] MD Del Curto et al, CRS 39th Annual Meeting & Exposition, Québec City, Canada, 15-18 July 2012.
[9] M Cerea et al, NCF 7, 114-117 (2002).
[10] A Gazzaniga et al, STP Pharma Sci 5, 83-88 (1995).
[11] H Tozaki et al, J Pharm Sci 86, 1016-1021 (1997).
[12] C Tuelu et al, Int J Pharm 180, 13-131 (1999).

MILD TECHNOLOGY FOR THE ENCAPSULATION OF CELLS

R. Dorati, B. Colzani, I. Genta, B. Conti
Dept. Drug Sciences, University of Pavia, Viale Taramelli 12, 27100 Pavia

Introduction

The cell trasplantation has been proposed to restore complex biological functions and to provide an endogenous and unlimited drug source for a particular therapy avoiding the need to regularly administer the drug to the patient. Over the past decades, different type of cells including primary cells, stem cells or bioengineered cells have been considered potentially therapeutic for the treatment of many diseases.
The cell encapsulation technology is a relatively old concept introduced almost 60 years ago, in the last decades different approaches have been proposed: microencapsulation, cell conformal coating, encapsulation in nano- and micro-fabricated devices and macroencapsulation. All the approaches began with a similar goal: to prevent the host immune system attack using a selectively permeable barrier [1].

Goal of the work

The purposes of this research project were to evaluate the feasibility of using the vibrational nozzle technology to encapsulate cells into polymeric beads and to characterized the cell loaded polymeric beads.

Experimentals

The polymeric beads made of alginate polymer (Pronova sterile alginate, G/M ratio ≥ 1.5, viscosity 100-300 mPa·s) were prepared by vibrational nozzle technology using Encapsulator B-395 Pro, Büchi. The process parameters (nozzle size, vibrational frequency, flow rate and electrostatic charge) were set up and optimized. Bead structure was analyzed by light microscope and scanning electron microscopy (SEM) to get images of bead surface before and after freeze-drying. The dimensional analysis were performed on fresh and freeze dried beads. The stability of the polymer membrane was assessed evaluating the rehydration and long-term resistance in KRH (pH 7.4), at 37°C supplemented with human plasma, and analysing the chemical and mechanical stability. Different molecules, as albumin and pullulans were used to evaluate the permeation capability and to determine the membrane cut off. The viability of cells encapsulated into the polymeric beads was evaluated by MTT assay. Cell loaded beads were freeze-dried using specific cryo-protectants (CPAs) mixtures and following the optimized freezing and rehydration protocols.

Results and discussion

Bead batches were prepared using a nozzle of 80 µm, and the optimized vibrational frequency (1500-2500 Hz) and the electrostatic charge (1300-1900 V). The morphological and dimensional characterization of batches #1-3 showed that the beads were spherical in shape with dimensions (d_{50}) ranged between 130-160 µm. After freeze-drying the beads appeared collapsed and minimally aggregated (**Figure 1**).

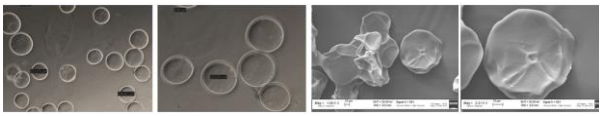

Figure 1 Light microscope and SEM images of microbeads (batch # 3) obtained by high efficiency vibration technique.

The hydration and long-term resistance studies demonstrated the capacity of freeze-dried beads to rehydrate gradually recovering the original spherical shape, no evidence of beads rupture was highlighted during the incubation. The polymeric beads resulted to be stable for 144 h in KRH (pH 7.4) supplemented with human plasma, at 37°C. Moreover, the chemical and mechanical tests demonstrated the good stability of the polymeric membrane in the sperimental conditions. The bead membrane resulted to be proper for the penetration of molecules with a 300 kDa cut off.
The preparation protocol set-up for the alginate beads was suitable for the encapsulation of cells, which present high viability both just after encapsulation and after short term incubation time (5 days).
The presence of CPAs into the freeze-drying suspensions increase the cell recovery after freezing: the freeze-drying suspension, composed of 30% (w/v) PVP40 + 20% (w/v) trehalose and cell loaded alginate beads, showed a cell viability of about 80%. Moreover, the rehydration protocol affects the cell viability percentages (**Figure 2**).

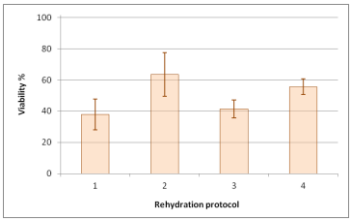

Figure 2 Effect of the rehydration protocols on cell viability: (1) 5 ml sol A gradually added, (2) 0,5 ml sol B/4,5 ml sol A gradually added, (3) 2 ml sol A (5 min)/6 ml KRH and centrifuge 6000 rpm and resuspended in 5 ml sol A and (4) 2 ml sol B (5 min)/6 ml KRH and centrifuge 6000 rpm and resuspended in 5 ml sol A. **Sol A**: DMEM +10% FBS and **sol B**: PVP40 (30%) + trehalose (20%).

Conclusion

The vibrational nozzle technology could be an useful technique to encapsulate cells into polymeric beads. Further studies are in progress to optimized the viability of cells after the freeze-drying.

References

[1] B. Nilsson, et al Trends in Immunology, 31(1), 32-38 (2010).

IN SITU FILM-FORMING SPRAY FORMULATION FOR THE IMPROVEMENT OF BUCCAL BIOAVAILABILITY OF DRUGS

F. Ferrari, M. Cicognani, S. Rossi, M.C. Bonferoni, G. Sandri, C. Caramella

Department of Drug Sciences, University of Pavia, Viale Taramelli 12, 27100 Pavia, Italy

Buccal administration of drugs intended for rapid and quantitative systemic absorption is often ineffective due to a too short residence time and to insufficient spreading on the absorption mucosa. when the actives are loaded in solid (sublingual tablets) or liquid (spray) formulations. This justifies the development of innovative liquid delivery systems to be easily sprayed on the buccal mucosa and to form *in situ* a mucoadhesive film, capable of withstanding the physiological removal mechanisms, thus improving bioavailability.

The aim of the present work was at first to optimize the composition of a liquid in situ film forming vehicle to be sprayed without propellant gas, and then to load such a vehicle with a model drug. Nitroglycerin, was chosen as model drug, since it must be rapidly and quantitatively absorbed in the mouth to achieve a prompt relief from acute attacks of *angina pectoris*.

Stock solutions of mucoadhesive film forming materials were prepared: 5% w/w Kollicoat® IR (PVA: PEG 75:25 w/w copolymer) in distilled water and 5% w/w Eudragit® S100 (polymethacrylate) in NaOH 1 M. A 3% w/w stock solution of NaCMC (Blanose®7LPH), chosen for its mucoadhesive properties, was prepared in distilled water. All solutions were adjusted to pH 7.2 ± 0.05.

Stock solutions were employed as such or mixed in predetermined w/w ratios to obtain the significant points (7) of a simplex centroid design [1]. The samples were characterized for viscosity at 25°C and at 37°C. Time for film forming was measured by spraying through a no-gas-pump a metered amount of each sample from a distance of 6 cm on a film prepared by drying a 8% w/w porcine gastric mucin dispersion in pH 6.4 phosphate buffer. The sample was placed in a thermostated (37°C) shaking (60 rpm) water bath and film formation was assessed by visual inspection. For spray area evaluation, each sample was delivered as above described on filter paper; the wet area was cut, dried and weighed and the weight was compared to that of a filter paper disc of known area.

Experimental data were treated with a statistical package, according to the experimental design chosen. The best fit model for all response variables (viscosity at $300s^{-1}$, time for film forming, spray area) was the special cubic one; it was predictive for all response variables ($p<0.05$). By superimposing the contour plots of each response variable the region of optimal composition of the vehicle, characterized by lowest viscosity at 25°C, highest viscosity at 37°C, lowest time for film forming, highest surface area, was found to be: Kollicoat® IR 1.60% w/w, Eudragit® S100 2.50% w/w, Blanose®7LPH 0.54% w/w.

Two medicated formulations were prepared by loading 0.25% w/w nitroglycerin (5% w/w in propylene glycol) either into the optimized vehicle (100% water) or into a hydro-alcoholic vehicle obtained by mixing in a 80: 20 v:v ratio the optimized vehicle with ethanol (96%).

Both medicated formulations and relevant vehicles were characterized for viscosity, time for film forming, spray area. Medicated formulations were characterized for mucoadhesion, evaluated by the inclined plane method [2] and drug release, determined after spraying in Petri plates (to allow partial film formation), adding pH 6.4 phosphate buffer and shaking the plates at 60 rpm and 37°C in a water bath. Nitroglycerin was assayed according to the USP 35 HPLC method.

Medicated formulations, packaged into amber-coloured glass bottles (20 ml) tightly closed by screw caps, were subjected to a preliminary stability study carried out in normal and accelerated ICH conditions up to 3 months.

Both medicated formulations and relevant vehicles are characterized by Newtonian behaviour at 25°C and 37°C. The medicated sample presents a slightly higher viscosity than the relevant vehicle. A significant viscosity increase characterizes all samples containing ethanol, indicating its worse solvent properties towards the polymers in comparison with pure water.

Whereas spray area is not affected by the presence of drug or by vehicle composition, time for film forming is significantly higher for samples (medicated or not) containing ethanol: this result is in line with the higher viscosity of these samples. Both medicated formulations are mucoadhesive, although mucoadhesion is more pronounced for the one not containing ethanol.

The release profiles of films, independently of the vehicle, are almost super-imposable; drug release rate is adequate to avoid withdrawal due to deglutition and to allow rapid drug absorption. Both formulations are stable when stored in normal conditions. A drug loss (~20%) occurs after 1 month storage at 40°C for the formulation not containing ethanol: this can be explained by the greater surface tension of pure water at the liquid/air interface, which favours drug evaporation in the headspace of the bottles. This loss keeps constant after 3 months and could therefore be overcome by a proper drug overload.

Thanks to the better film forming and mucoadhesive properties, the formulation based on the vehicle of optimized composition, not containing ethanol, represents the more promising candidate for the administration of drugs, like nitroglycerin, that are intended for a rapid and quantitative buccal absorption, after spraying through a no-gas pump and *in situ* film formation.

REFERENCES

[1] Ferrari F. et al., *Pharm. Dev. Tech.*, 1, 159, (1996)

[2] Sandri G. et al., *Curr. Drug Discov. Technol*. 8, 277 (2011)

NOVEL pH RESPONSIVE POLYMERIC VESICLES FOR siRNA DELIVERY TO THE TUMOR

E. Gallon[1], S. Salmaso[1], F. Mastrotto[1], S. Bersani[1], J. Sanchis[2], M.J. Vicent[2], G. Mantovani[3], T. Matini[3], C. Alexander[3], P. Caliceti[1]

[1]Dep. of Pharmaceutical Sciences, University of Padua, Via F. Marzolo 5, 35131, Padua, Italy. e-mail: stefano.salmaso@unipd.it [2]Polymer Therapeutics Lab., Centro de Investigación Príncipe Felipe (CIPF), Av. Autopista del Saler 16, 46012 Valencia, Spain. [3]School of Pharmacy, University of Nottingham, Nottingham NG7 2RD, U.K.

ABSTRACT SUMMARY

Triblock pH-responsive co-polymers were synthetized by RAFT polymerization and assembled in vesicles for the delivery of siRNA to cancer cells. The copolymers self-assemble in spherical shape vesicles at pH 7.4 with a size of 60 nm, high homogeneity and good stability at 37°C. The carrier loads double stranded DNA sequences with a 14% molar loading capacity and release the payload in 8 hours at pH 5 while at pH 7.4 the release was negligible. The vesicles possess remarkable hemolytic activity at pH 5 which can be correlated with potential endosome escape of the system. Polymeric vesicles decorated with folate showed a selective cell association with a model cancer cell line overexpressing the folate receptor.

INTRODUCTION

In the last decades a variety of supramolecular systems obtained by self-assembly of functional polymers have been developed with the aim of preserving the therapeutic activity of loaded drugs whilst reducing their side effects. However, these nanocarriers lack targeting modalities and the ability to perform sequential operations needed to achieve controlled release of the drug at the biological target. These limitations can be overcome by using nanosystems with both biorecognition capacity and the responsive behavior to peculiar environmental stimuli.

The aim of this study was to synthesize and investigate pH responsive triblock copolymers able to assemble into targeted vesicles for siRNA delivery to cancer cells. Folic acid was chosen to confer active targeting for the biorecognition of folic acid receptor over-expressing tumor cells [1]. Once endocytosed by the target cells, the pH responsive vesicles can disassemble in the endosomes by protonation of ionizable monomers of the co-polymers and release the siRNA.

EXPERIMENTAL METHODS

Synthesis of triblock copolymer mPEG$_{1900}$-poly(C_6-imidazoyl-methacrylate-co-gliceroyl-methacrylate) (**1**) The co-polymer was synthetized by a three steps procedure: **a)** mPEG-OH was reacted with 4-cyano-4-(phenylcarbonothioylthio)-pentanoic acid (CPAD), in the presence of DMAP and DCC to obtaine a macro-transfer agent (macro-CTA); **b)** *C_6-imidazoyl-methacrylate* was polymerized using the macro-CTA according to a RAFT polymerization procedure; 3) mPEG-poly(C_6-imidazoyl-methacrylate) was then used to polymerize glyceroyl-methacrylate by RAFT polymerization (see Scheme 1 for chemical structure).

Synthesis of t-Boc–NH–PEG$_{3500}$-poly(C_6-imidazoyl methacrylate-co-gliceroyl-methacrylate) (**2**). The co-polymer was synthetized as reported for (**1**) using t-Boc-NH-PEG-OH as starting material.

Synthesis of folate–NH–PEG$_{3500}$-poly(C_6-imidazoyl methacrylate-co- gliceroyl-methacrylate) (**3**). Polymer (**2**) was treated with a 1:1 (v/v) CF_3COOH/DCM mixture to remove the Boc agent; the unprotected polymer was isolated by solvent evaporation and reacted with N-hydroxysuccinimidyl ester activated folic acid in DMSO. The crude product was purified by dialysis using a 3.5 kDa cut-off dialysis bag (see Scheme 1 for structure).

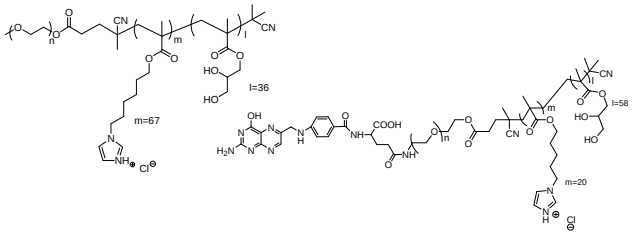

Scheme 1. Chemical structure of triblock copolymers (**1**) on the left and (**3**) on the right.

All polymers were characterized by ^{1}H-NMR, GPC, potentiometric titration, turbidimetric and Photon Correlation Spectroscopic (PCS) analysis.

Vesicles assembly. Targeted vesicles were assembled using a 90:5:5 w/w ratio of polymers (**1**)/(**2**)/(**3**). Control untargeted vesicles were prepared with a 90:10 w/w ratio of polymer (**1**)/(**2**). The vesicles were assembled by dissolving 1 mg/ml of the copolymers in PBS at pH 3 and increasing the pH to 7.4 using 0.1 M NaOH. The vesicles formation was confirmed by PCS.

Kinetic stability studies. The stability of 1 mg/ml vesicles was performed by analyzing the size evolution over time with PCS. The investigation was carried out in PBS at pH 7.4 at 37°C with and without foetal bovin serum.

DNA loading and release. A Tris buffer solutions of 19-mer oligomeric dsDNA (100 μM) was added to polymer mixtures in PBS at pH 4 to achieve a 10:1 and 1:1 N/P ratio. Polymer mixtures had the same composition reported above to obtain targeted and untargeted vesicles. Polymers were then induced to assemble by the pH increase method. The dsDNA loading yield and release from the nanocarrier was at 37°C at pH 7.4 and 5.0 by Uv-Vis spectroscopy.

TEM images. dsDNA-free and dsDNA-loaded polymersomes were analyzed by TEM in negative staining mode and the contrast staining was performed with a 1% w/v uranyl acetate solution.

Hemolytic assay. The hemolytic activity of polymers was evaluated on erythrocytes at polymer concentrations ranging from 0.5 to 5.0 mg/mL at pH 7.4, 6.5, 5.5.

In vitro cell uptake studies. Targeted and untargeted vesicles loaded with rhodamine-6G labelled dsDNA were incubated with KB cell that overexpress the folate receptors and MCF-7 cells that do not express the folate receptor for 1 hours at 37°C and cells were then analyzed by cytofluorimetry.

RESULTS AND DISCUSSION

The novel pH responsive copolymers showed a pK_a of 6.5. This property allows for deprotonation of the imidazoyl monomers at neutral pH, which increase the hydrophobic character of the polymer central block and promote the self-association of the carrier. At acid pH the imidazoyl monomers are in the protonated state and the polymer central block become more hydrophilic allowing for dissociation of the vesicles in acidic conditions such as those found in endosomes and lysosomes [2]. The copolymers self-assemble in vesicles at pH 7.4 with a size of 60 nm and are very stable at room temperature. At 37°C the stability of the vesicles can be modulated by increasing the ratio of the copolymer (**2**).

The vesicles were loaded with a model oligonucleotide. The carrier loads the dsDNA very efficiently with a 14% molar loading capacity. DLS analysis revealed that the dsDNA loaded vesicles arrange in slightly larger systems compare to empty vesicles with a mean diameter of 230 nm. The empty and loaded vesicles showed a spherical shape and high size homogeneity (Figure 1).

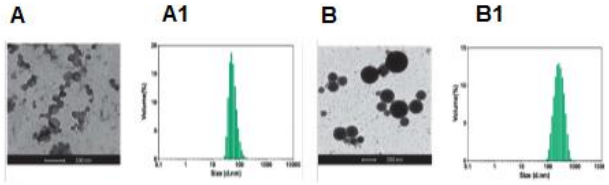

Figure 1. TEM images (A and B) and DLS analysis (A1 and B1) of empty (A, A1) and DNA-loaded (B, B1) vesicles.

The dsDNA release study was performed in pH conditions mimicking the systemic circulation and the late endosomal/lysosomal intracellular compartments. As reported in Figure 2, release of the dsDNA was markedly pH-dependent, with 85% of the encapsulated nucleic acid released at pH 5.0 after 8 h, whilst only 15% of entrapped dsDNA was released by the nanocarriers at pH 7.4 over the same time.

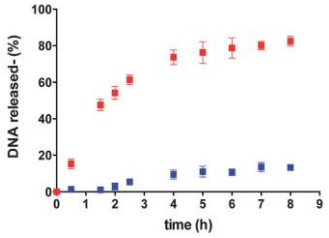

Figure 2. Kinetics of dsDNA release from polymersomes at pH 5 (■) and 7.4 (■).

The ability of the carrier to escape the endomal compartment was evaluated with a dedicated hemolytic assay. The polymers at 0.5 and 1.5 mg/mL does not induce hemolysis at pH 7.4, which proves the hemocompatibility of these materials. However, at pH 5.5 the copolymers showed a hemolytic activity of about 60-70% with respect to polyethylenimine (PEI) used as positive control at all concentration tested which can be correlated with the endosomal escape ability of the carrier.

The uptake of folate targeted vesicles loaded with fluorescently labelled dsDNA was five time higher for KB cells as compared to MCF-7 cells, and 2.4 time higher as compared to untargeted carrier confirming that vesicles are taken up by cells via a receptor-mediated process (Figure 3).

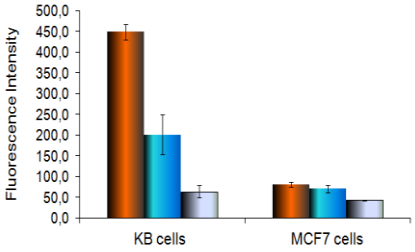

Figure 3. Cellular uptake profile after incubation of cells with untargeted polymersomes (■) and targeted polymersomes (■).

CONCLUSIONS

The novel pH-sensitive copolymers proposed in this study spontaneously assemble in nanosized vesicles that disassemble at lower pH for site-specific endosomal release of loaded drugs. The vesicles have good stability at physiological conditions and load efficiently small oligonucleotide sequences that are released at low pH mimicking the endosomal environment. The copolymers possess a sharp response and adequate behavior for the endosomal escape, and are able to selectively deliver oligonucleotides into specific cancer cell lines via a receptor-mediated uptake pathway.

REFERENCES

1. Dosio, F.; Arpicco, S.; Stella, B.; Brusa, P.; Cattel, L. (2009) Int. J. Pharm. 382, 117-123.
2. E. S. Lee, Z. Gao and Y. H. Bae, (2008), J. Controlled Release 132, 164-170.
3. N. Murthy , J. R. Robichaud , D. A. Tirrell , P. S. Stayton , A. S. Hoffman. (1999) J. Control Rel. 61 137-143.

ACKNOWLEDGMENTS

This project (acronym INANONAK) is part of ERANET NanoSci-E+ and was financially supported by Italian CNR, british EPSRC, Spanish MICINN (EUI2008-03905) and by the European Commission.

IN VITRO RELEASE STUDIES FROM CURCUMIN-LOADED INULIN-GRAFT-VITAMIN E (INVITE) MUCOADHESIVE MICELLES

[1]Delia Mandracchia, [2]Giuseppe Tripodo, [1]Andrea Latrofa

[1]Department of Pharmacy, University of Bari "Aldo Moro", Via Orabona 4, 70125 Bari, Italy
[2]Department of Drug Sciences, University of Pavia, Viale Taramelli 12, 27100 Pavia, Italy

Introduction

The term urinary tract infections (UTI) is used for any infection occurring in the urinary tract. They affect a wide range of the population and are associated with high healthcare and social costs. Most of the UTIs are treated with antimicrobial agents with a high spectrum of activity and, often, this lead to antimicrobial resistance and other side effects, so the research of new site specific formulations is an important challenge in the treatments of UTI [1, 2]. This is why there is a great interest to find appropriate formulations to solve this problem.
Vitamin E (VITE) shows several beneficial effect toward urinary tract affections and its consequences such as oxidative stress, so, being used as adjuvant in UTI therapy [3, 4], but VITE is slightly water soluble, high lipophilic and oxidizable determining, by a pharmaceutical technology point of view, some formulation issue. In this context, polymers are interesting materials for the modern pharmaceutical technology, that allow the obtainment of advanced Drug Delivery Systems (DDS). Taking into account the above considerations we studied a strategy to obtain a new formulation able to release hydrophobic drugs in the urinary tract and we selected Inulin (INU), a non-toxic, biocompatible, water soluble, biodegradable, very cheap and FDA approved polymer, as a polysaccharide compound to form Inulin-graft-Vitamin E amphiphilic polymers. Inulin is also known because it is totally filtered by kidney and it is not secreted or reabsorbed at any appreciable amount at the nephron where it can accumulate. This unique behaviour of Inulin,can induce a passive targeting of the obtained micelles in the urinary tract after intravenous administration. Moreover, a so ideated system should solubilize, incorporate and protect lipophilic drugs while delivering them. In this work, we prepared three different polymeric inulin-graft-Vitamin E (INVITE) micelles by using INVITE conjugates with three different degree of derivatization in vitamin E. INVITE micelles were loaded with curcumin, chosen as a lipophilic drug potentially useful as an antioxidant agent for UTI therapy, by using two different technique of incorporation in order to compare the corresponding drug loading values.
Then, micelles were characterized for their mucoadhesion properties and by *in vitro* release studies of curcumin in simulated physiological conditions.

Aim of the work

In order to investigate the potential use of INVITE micelles for urinary tract infections, we tested the ability of INVITE micelles to entrap and release a hydrophobic model drug such as curcumin, known for its high antioxidant properties and we evaluated the micelles mucoadhesive properties.
In particular, micelles from INVITE polymers, at different degrees of substitution in VITE (10, 20 and 40%), have been prepared by the direct dialysis method so obtaining three different micelle systems.
The same systems have been further drug loaded with curcumin by using two different methods in order to evaluate the influence of loading methods on drug loading capacity. *In vitro* drug release studies and mucoadhesive properties in simulated physiological conditions were carried out aimed to verify whether this DDS could be good candidate for the treatment of UTI.

Experimentals

Inulin-α tocopherol conjugates (INVITE) were synthesized at different degree of substitution in VITE. Briefly, vitamin E succinate (1 eq) was dissolved in DMF and DCC (2 eq) and NHSS (2 eq) were added. Then, INU and TEA were added and the reaction, according to a molar rate VITE/INU 0.1, 0.2, 0.4 was carried out under nitrogen at 25 °C for 24 h and the INVITE polymers recovered from acetone.
Drug loading was performed by two different methods, the direct dialysis from DMSO and the O/W emulsion technique.
For drug loading by direct dialysis, 100 mg of INVITE were solubilized in 10 ml of DMSO, then 3 mg of curcumin were added. After complete solubilization, the solution was poured in a dialysis tube with a MWCO 3.500 Da and dialyzed against water for 3 days. The clear/yellow solution has been lyophilized and recovered with 86 % w/w yield with respect to the starting polymer. The same method, without drug, was used for the formation of not drug loaded INVITE micelles. For drug loading by O/W emulsion technique 3 mg of curcumin was dissolved in 1 mL of DCM and this solution was added under constant stirring, ultraturrax for 2 min at 11.000 rpm, to 5 mL aqueous micellar dispersion. The clear/yellow dispersion was stirred overnight, then was filtered through 0.45 μm

filter membrane to remove non-incorporated drug,lyophilized and recovered with 98 % w/w yield with respect to the starting polymer.
Curcumin drug loading was determined by UV-VIS after solubilization of curcumin loaded micelles in DMSO. Drug loading coefficient (DL wt%) was calculated based on the following formula:

DL (wt%) = weight of curcumin in micelles / weight of the feeding micelles and curcumin x 100%

Curcumin release studies were performed *in vitro* in phosphate buffered saline (PBS) pH 7.4 plus 0.5% Tween 80, in phosphate buffered saline (PBS) pH 5.5 with 0.5% Tween 80 or in simulated urine pH 5.5. Briefly, the solutions (10 mg/mL) of curcumin-loaded INVITE micelles were placed into dialysis tube with a MWCO 3.500 Da and dialyzed against 10 mL of the appropriate release medium at 37°C and 100 rpm. Then, at predefined time intervals, the release medium was collected and replaced with an equal volume of fresh pre-warmed release medium. The amount of curcumin released was evaluated by UV-VIS and calculated by a calibration curve.
The INVITE micelles were also characterized in terms of mucoadhesive properties. Briefly, mucin (10 mg) was dispersed in PBS (pH 5.5) (10 ml) and the mixture was kept at 37°C for 24 h under stirring (100 rpm). Then, appropriate amounts of INVITE micelles or poly(acrylic acid) (chosen as a positive control) were incubated with the mucin dispersion at 37°C under stirring (100 rpm) for 2, 5, 8, 15 or 24 h. After each incubation time, the transmittance (%) of the samples was recorded at 650 nm.

Results and discussion

In this study, we compared two different drug loading mechanisms for hydrophobic curcumin drug into INVITE micelles prepared from three different INVITE conjugates.
Between these methods the direct dialysis technique was superior in terms of drug loading respect to the O/W emulsion technique. The reason of this observation could be attributed to a better dispersion of the drug during the micelle loading due to a slow displacement of the DMSO that allowed the drug being incorporated before its precipitation in water.
In vitro drug release studies showed a controlled slow release of curcumin in simulated physiological media. In particular only a slight amount of curcumin was released up to 48h in PBS pH 7.4, meanwhile the curcumin release increased in simulated urine at pH 5.5.
Mucoadhesive properties of INVITE micelle, evaluated by a turbidimetric method, showed that transmittance values for INVITE micelles are lower than those found for poly(acrylic acid), therefore, the micelles show an interaction with mucin stronger than that of the positive control. Moreover, it was evident that the transmittance value of INVITE 2 and INVITE 3 micelles became about constant after 8 h of incubation with mucin, and INVITE 1 micelles after 24 h, thus suggesting that the maximum polymer–glycoprotein interaction is reached at different time, depending of the different degree of derivatization in VITE of the starting conjugate.
Taking into account the *in vitro* drug release results and the mucoadhesive behavior of INVITE micelles it is reasonable to suppose that INVITE micelles could be potentially useful for a site-specific prolonged delivery at the urinary tract .

Conclusions

These preliminary results show that INVITE micelles are able to incorporate hydrophobic drug curcumin with different technique and to release it in a prolonged way. These results, together with the high mucoadhesive properties of the INVITE micelles make them good candidate for use in the urinary tract infection therapy.

References

[1] T.E.B. Johansen, H. Botto, M. Cek, M. Grabe, P. Tenke, F.M.E. Wagenlehner, K.G. Naber, International Journal of Antimicrobial Agents, 38 (2011) 64-70.
[2] L.A. Beveridge, P.G. Davey, G. Phillips, M.E.T. McMurdo, Clinical Interventions in Aging, 6 (2011) 173-180.
[3] M.J. Fryer, Nephrology, 5 (2000) 1-7.
[4] E. Haugen, K.A. Nath, Blood Purification, 17 (1999) 58-65.

SOLID LIPID NANOPARTICLES LOADED WITH A NEW CODRUG FOR ALZHEIMER'S DISEASE

L. Marinelli[1], S. Laserra[1], A. Basit,[2] P. Sozio[1], Hasan Türkez,[3] A. Di Stefano[1]

[1]Department of Pharmacy, "G. D'Annunzio" University, Via dei Vestini 31, 66100 Chieti, Italy.
[2]Department of Pharmaceutics, UCL School of Pharmacy, University College London, WC1N 1AX, London, UK.
[3]Department of Molecular Biology and Genetics, Erzurum Technical University, Erzurum 25240, Turkey.

Alzheimer's disease (AD) is the most common progressive age-related neurodegenerative disease characterized by progressive loss of memory and cognition and profound neuronal loss [1]. Various strategies have been developed to prevent or mitigate the progression of AD. In our previous work we covalently linked memantine (3,5-dimethyl-1-adamantanamine, MEM)) with (R)-a-lipoic acid (LA) and this new lipophilic compound (LA-MEM) seemed to be a promising drug candidate in pathological events such as AD where both free radical damage and inflammatory activity in the brain are involved [2]. In order to overcome the challenges associated with oral drug delivery, solid lipid nanoparticles (SLNs) have emerged as suitable drug delivery systems (DDS).

Starting from these data, we prepared SLNs loaded with LA-MEM according to the emulsification-evaporation-solidifying method [3]. These loaded SLNs were formulated with different drug:lipid ratio (1:20, 1:10, 1:5 and 1:2.5) and properties, such as intensity average diameter, polydispersity indices, zeta potential, yield and entrapment efficiency, were evaluated for each formulation.

It was found that the size of loaded SLNs was slightly higher than that of drug-free one due to the incorporation of drug into the particles matrix.

The different formulations didn't show significant changes in yield, zeta potential and entrapment efficiency.

On the basis of the particle size and PDI values the formulation with 1:5 drug:lipid ratio was chosen as the optimal formulation and its stability was investigated, after the incubation in the simulated gastric fluid (SGF, pH 1.2 with and without pepsin) and in the simulated intestinal fluid (SIF, pH 6.8 with and without pancreatin). The particles seemed stable in the gastric environment, because no significant aggregation was detected by dynamic light scattering: after 2 h of incubation the size and the PDI were maintained. In the contrary, the particles are subjected to aggregation phenomena in the intestinal media.

The in vitro release profile was also evaluated in sink conditions in simple SGF and SIF without enzymes and in the presence of Cremophor ELP 0.1% v/v [4]. The results indicated that in both media, a small burst release in the first hour was present, followed by a more sustained trend. In particular, in the gastric and intestinal simulated fluids, after 2 and 4 h respectively, approximately only 20% of the compound was released. Thus it is reasonable to assume that the particles may be absorbed before a considerable amount of the drug is released in the gut, improving its bioavailability.

In this present study we also tested the cytotoxicity potentials of newly synthetized SLN formulations in different in vitro cell models for establishing the possible loaded SLNs suitability or limitations. Therefore, the cytotoxicity was tested in mouse N2a neuroblastoma (NB) and primary human whole blood (PHWB) cells [5]. Cell viability and cell membrane damage was determined using the MTT and lactate dehydrogenase (LDH) assays, respectively. Total antioxidant capacity (TAC) and total oxidative stress (TOS) levels were also determined to assess the oxidative alterations.

The cultured PHWB and N2a NB cells exposed to 10 µM concentrations of loaded SLNs did not show any significant changes in cell viability during 24 h wherease at a concentration of 100 µM a slight toxicity was observed. Furthermore, the TAC and TOS levels were similar in 100 µM loaded SLNs treated and untreated cultures.

At this point, present cytotoxicity and oxidative damage analyses revealed that SLNs loaded with the LA-MEM codrug could be used as a suitable and safe DDS for the brain, from a toxicological perspective.

References

[1] Brookmeyer, R. et al. Alzheimers Dement. 2007, 3, 186–191.
[2] Sozio P. et al. Eur. J. Pharm. Sci. 2013,49, 187–198.
[3] Shahgaldian P. et al. Int. J. Pharm. 2003, 253, 23-38.
[4] Verger M.L.L. et al. Eur. J. Pharm. Biopharm. 1998, 46, 137-143.
[5] Coleman N. et al. Pharmaceuticals 2013, 6, 536-545.

INFLUENCE OF THE CURING PROCESS ON THE CONTROLLED RELEASE COATING OF PELLETS PREPARED IN A WURSTER FLUID BED

C. Melegari[1], A. Genovesi[2], M. Di Sabatino[1], N. Passerini[1], B. Albertini[1]

[1]University of Bologna, Department of Pharmacy and BioTechnology
[2] Colorcon® Italia

Due to several biopharmaceutical advantages for oral delivery, modified release multiple unit dosage forms are more effective therapeutic alternative to the single units systems. When multiple unit systems are orally administrated, they maximize absorption, minimize side effects, empty gradually and predictability from the stomach even in presence of food and reduce inter-and-intra subject variability in oral bioavailability. Moreover, with emerging interest in personalized medicine, they are suitable for individualized dosing.

These systems may exists as pellets, granules, minitablets and microparticles with their final application form as an oral suspension, sachet, tablet or capsule.

Pelletization techniques are mainly based on extrusion / spheronisation, direct pelletization in a rotor fluid bed or in a high shear mixer granulator and pelletization by solution / suspension or powder layering in a Wurster fluidized bed coater [1]. While the latter equipment is fairly established and widespread in pharmaceutical industry, a lot of studies, including Quality by Design and troubleshooting investigations, are necessary to cope with the numerous issues that arise during formulation development [2].

The research project is aimed to investigate the whole process of production of multiple unit pellet systems in a Wurster fluidized bed coater for oral drug delivery.

Pellets have been prepared by drug layering and film coating, focusing on both formulation variables and process related – parameters that may influence drug release. A mucolytic drug, used for the treatment of acute respiratory tract infection symptoms, has been selected as a suitable model soluble API (BCS class I) for formulating extended release systems.

The first part of the work has focused on the drug layering process onto starting beads (sugar beads, based on sucrose and starch) using a suitable binder-layering solution.

The API was layered onto 600 – 710 µm Suglets ® in a mini-Glatt fluidized bed coater equipped with a Wurster column, using Methocel E5 solution layering (5% w/w). Differential Scanning Calorimetry (DSC), Hot Stage Microscopy (HSM) and Scanning Electron Microscopy (SEM) were used to investigate and characterize the solid state of the API after the process.

In the second part of the study , the drug loaded pellets have been coated using Surelease®, a suitable aqueous ethycellulose dispersion specifically designed for controlled release. The process was stopped after spraying polymer blend equivalent to 12% of the theoretical weight gain (w/w expressed as percentage of total mass). The influence of process parameters on the coating efficiency (RSD_C%) of the process was investigated [3].

Since a complete polymer particle coalescence is difficult to be assured during the coating process, a curing step is usually recommended. Indeed, a post–coating thermal treatment was performed both under static conditions in an oven (at 40°C and 60°C for 2 hours) and under dynamic performances using either a solid wall pan coater (at 60°C for 2 hours) or the fluid bed coating equipment (at 40°C and 60°C for 2 hours).

In vitro dissolution testing (USP Apparatus 2 dissolution system) has been used to investigate the release performance. The dissolution profiles obtained from uncured and cured samples have been compared using the similarity factor f_2 in order to evaluate the effect of curing conditions (type, time and temperature) on the reproducibility of the drug release. Finally, the stability of uncured/cured samples has been evaluated (T =25°C, RH= 60% and t=90 days).

The results of the layering process evidenced a drug loading of 4,65 (±0,08) % w/w and a yield process of 98,5%. Based on 4 batches, the layering efficiency was 3.90%. The drug is freely soluble and the 85% of the dose was dissolved within 2 min. The complete dissolution of the drug from the layered product occurred in 15 min. After the coating process, the real drug content was lowered to 4,10 (±0,25)% w/w due to the weight gain of 13.36%. Also for this process, the yield was high (98.4%). SEM analysis revealed the API's crystal growth onto the surface of the coated pellets. The coating process significantly decreased the drug release and about the 80% of the API was dissolved after 180 min, indicating the efficiency of the coating process.

As regards the curing conditions in the fluid bed equipment, no significant differences of the release profiles between the cured and uncured pellets were observed, both at t_0 and t_{90}, indicating the stability of the ethylcellulose-based coating of both untreated/ treated samples.

Looking inside to the solid state of the drug throughout the whole process (layering, coating and curing), it was noticed during DSC analysis the appearance of a new endothermic peak in the layered pellets, attributable to the API polymorphic form. This fact was also suggested by the HSM pictures. The DSC scans of the uncured and cured t_0 samples showed only one broad endothermic peak, which comprises several thermal events (Tg of the polymer, API main melting peak and API polymorphic endotherm) non-distinguishable. Analyzing the stored samples (t_{90}), the splitting of the main endotherm was observed both in the layered and in the uncured pellets, while it didn't appear in the cured t_{90} samples. This behavior indicate the better

stability of the cured pellets with respected to the untreated ones.

After 2 hours of curing at 40°C in oven, the release profiles of uncured and cured pellets were similar both at t_0 and t_{90}. However the data are more variable and an higher burst effect of cured t_{90} sample was clearly observed.

When pellets were cured for two hours at 60°C, it was impossible to perform the process in the fluid bed, as samples softened along with the pellets de-fluidization, due to the Tg of the polymer/plasticizers blend around 62°C. Therefore the coating pan equipment was used to assess the dynamic curing.

The effect of the curing conditions in the coating pan revealed a different behaviour of the pellets, especially during storage. After 90 days the release profile of the cured pellets shows a significant burst effect and an increase of the API released, probably due to the trigger of the API migration through the coating level. The solubility of the API was very sensitive to the process temperature and while at 40°C it was partially dissolved into the polymer mixture, at 60°C it was completely dissolved.

When the curing is performed under static conditions at 60°C, the release profiles of the uncured and cured samples were similar at t_0. After 90 days of storage, the release profiles of uncured t_0 vs cured t_{90} were significantly different; while the release profiles of uncured t_{90} vs cured t_{90} were borderline different (f_2 = 47). This behavior was confirmed by the difference factor value (f_1= 22), calculated after the release of the 50% of the dose. Therefore the enhanced API release after the thermal treatment in oven at 60°C is less pronounced than in the coating pan at 60°C, but still present.

In conclusion, the results revealed the better dynamic curing performances on the API stability with respect to static thermal treatment when performed at a suitable temperature. Actually, the Tg of aqueous ethylcellulose pseudolatex, the API melting point and the drug solubility into the polymeric coating displayed an important role on the curing process and thus on the controlled release of the pellets.

References:

[1] Encyclopedia of pharmaceutical technology, New York, NY: Marcel Dekker, Inc. (1997).

[2] ICH Harmonised Tripartite Guideline, Pharmaceutical Development Q8. (2008).

[3] McGinity J.W., L.A. Felton, Aqueous Polymeric Coatings for Pharmaceutical Dosage Forms. 3rd Ed. Informa Healthcare, New York (2008).

DEVELOPMENT AND CHARACTERIZATION OF OPIORPHIN LIPOSOMAL

Natascia Mennini[1], Paola Mura[1], Cristina Nativi[1], Barbara Richichi[1], Carla Ghelardini[2]

[1]Department of Chemistry and [2]Department of NEUROFARBA, University of Florence

Introduction

Opiorphin is a natural peptide secreted into human saliva that shows a strong analgesic effect, even superior to that of morphine [1]. It acts as an inhibitor of pain perception by potentiating the endogenous enkephalin-releated via activation of μ- and δ-opioid pathways. [2,3]. Moreover, pharmacological data suggest other possible clinical applications of this promising peptide which, over antinociceptive activity, showed anticraving, antidiarrheal and antidrepressant properties [4-6]. Moreover, since opiorphin does not activate directly the opioid receptors, many side effects given by morphine and morphine-like drugs should be mitigated. However, despite the strong pain-killing activity of opiorphin, its short duration of action can be considered an obstacle to its successful use into clinical practice. It has been suggested that a possible reason of this effect could be a rapid degradation by the peptidases in the bloodstream [1].

Goal of the work

On the basis of all these considerations, the purpose of the present research project was to develop a suitable delivery systems, able to protect opiorphin from degradation, after its intravenous administration, thus ensuring a prolonged analgesic action of the peptide. With this aim, both conventional and "stealth" liposomes loaded with opiorphin were prepared and fully characterized.

Experimentals

Conventional liposomes (CL) were prepared according to the film hydratation method. The lipid phase (Phosphatidylcholine, cholesterol and stearylamine) was dissolved in chloroform in a round-bottomed flask; the organic solvent was then removed under vacuum and the obtained dry lipid film was hydrated, under stirring, with 10 ml of physiological solution where opiorphin was previously dissolved (1 mg/ml). The hydrated film was then subjected to a water bath heating at 58 °C (5 min) and vortexing (1 min) repeated 3 times.

Preparation of the PEGylated liposomes (PL) differed from that of conventional liposomes only for the addition of PEG (2000)–DSPE (2 mg/ml) to the lipid phase. Opiorphin was assayed by high-performance liquid chromatography (HPLC) analysis.

All liposomal formulations were characterized for particle size, polydispersity index (PDI) and Zeta potential by Photon Correlation Spectroscopy.

The morphological characteristics of the vesicles were examined by Transmission Electron Microscopy

Encapsulation efficiency (EE%) was determined after separation of free opiorphin from loaded liposomes by gel permeation chromatography.

Physical and chemical stability of conventional (CL) and stealth PEGylated liposomes (PL) loaded with opiorphin was checked for 3 months.

The antinociceptive effect of the opiorphin liposomal formulations was evaluated in vivo on rats by the tail flick test and compared with that of a simple aqueous solution of the peptide at the same concentration.

Results and discussion

The results of characterization of opiorphin liposomal formulations in terms of size, polidispersity (Pd) and Zeta potential are summarized in Table 1. The mean diameters of all opiorphin-loaded vesicles was less than 230 nm, thus resulting suitable for intra-venous (i.v.) administration. Moreoever, the particle size further decreased by addition of PEG into the liposomal membrane (228.8 nm vs. 163.9 nm). This could be explained by a steric stabilization of the vesicles due to the presence of the PEG chains, that reduce feasible aggregation phenomena of liposomes, resulting in their smaller mean size. As a further confirmation of this hypothesis, the polydispersity index of PEGylated liposomes (Oph-PLs) was less than 0.2, indicative of a well homogeneous size distribution, while the dimensions of conventional liposomes (Oph-CLs) resulted more polydisperse (PDI=0.316).

Finally, Oph-CLs showed a positive Zeta-potential value due to the presence of stearylamine molecules into the vesicle membrane. On the contrary, in the case of Oph-PLs, the negatively-charged phosphate groups of PEG-DSPE chains counterbalanced to a great extent the positive charges of stearylamine molecules, leading to a slightly negative value of Zeta potential.

Table 1: Size, polydispersity index (PDI) and Zeta potential values of opiorphin liposomal formulations (mean ±S.D., n=5).

Sample	Size (nm)	PDI	ζ-potential (mV)
Oph-CLs	228.8±21.8	0.316±0.035	+14.7±3.4
Oph-PLs	163.9±1.5	0.195±0.009	-0.62±0.13

The images obtained by Transmission Electron Microscopy (TEM) showed that the vesicles of both conventional and PEGylated liposomes were of discrete and round structure. In the case of liposomes

associated with DSPE-PEG2000, a white coated film was observed on the vesicle surface.

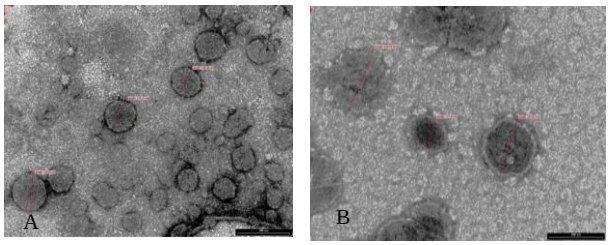

Fig 1: Trasmission Electron Micrographs of opiorphin-loaded conventional (A) and PEGylated (B) liposomal dispersions

The opiorphin loading efficiency for conventional and PEGylated liposomes was found to be 75.7% and 95.2%, respectively.
Stability studies demonstrated that the mean size of all liposomal dispersions remained almost unchanged over 3 months. In particular, the vesicle size variations were up to 12 % and 11 % of the original values for conventional and PEGylated liposomes respectively. Furthermore, also the polydispersity was stable during time.
In vivo studies were carried out to assess the actual efficacy of the liposomal formulations.
The significant increase in the intensity and duration of the analgesic action obtained by i.v. administration on rats of opiorphin-loaded PEGylated liposomes, with respect not only to simple opiorphin physiological solution but also to opiorphin-loaded conventional liposomes, confirmed the effectiveness of PEGylated liposomes in protecting the drug from enzymatic degradation, thus enabling the achievement of a prolonged pain-killing effect.

Conclusion

These preliminary results clearly showed that PEGylated liposomes proved to be a better a more efficent carrier for opiorphin with respect to conventional liposomes, and they could be considered a promising approach for allowing a successful use of the peptide into clinical practice.

References

[1] Tian X. et al., Peptides 30, 1348–1354 (2009).
[2] Wisner A. et al., Proc. Natl. Acad. Sci. U.S.A. 103, 17979-17984 (2006).
[3] Rougeot C. et al., J. Physiol. Pharmacol. 61, 483-90 (2010).
[4] Thanawala V. et al., Current Drug Targets 10, 887-894 (2008).
[5] Javelot H. et al., J. Physiol. Pharmacol. 61, 355-623 (2010).
[6] Qing Z.Y. et al., . Neurosci. Lett., 489, 131-135 (2011).

ULTRASOUND AND 3D SKIN IMAGING: METHODS TO EVALUATE SKIN GRAFTING RECOVERY

[1]Mariella Bleve, [2]Tommaso Pellegatta, [3]Priscilla Capra, [2]Giovanni Nicoletti, [2]Angela Faga, [3]Franca Pavanetto, [1,3]Paola Perugini

[1] EticHub s.r.l.,Department of Drug Sciences, via Taramelli 12, [2]Plastic Surgery Unit, University of Pavia, Salvatore Maugeri Research and Care Institute, via Maugeri 8-10, Pavia, Italy, [3]Department of Drug Sciences, University of Pavia, via Taramelli 12, 27100 Pavia, Italy

Introduction. Because there are different types of wounds, treatment should be selected individually for each defect after consideration of all closure. When selecting a technique to cover a wound, the major goal is to restore the functional integrity of the skin with the best possible aesthetic outcome.

Skin graft, generally classified as split-thickness or full-thickness grafts, is one of the most indispensable techniques in plastic surgery and dermatology. Skin grafting is commonly used for the treatment of burns and has become a popular method for treating chronic ulcers and skin defects caused by removal of cutaneous malignancies. The past decade has seen the emergence of tissue engineering as an increasingly more viable alternative for skin replacement. Artificial skin is considered beneficial for 'difficult-to-heal' chronic venous-ulcers, as well as for acute wounds such as burns and reconstructive wounds [1-.

Aim of the work. The aim of this study is to evaluate if ultrasonography and 3D visualization techniques can be used to obtain an objective assessment of physiological bases concerning the functional and aesthetic recovery of the skin grafting. In particular, the correlation between the mechanisms that occur in the deeper layers of the skin and the appearance of skin surface texture was investigated. The ultimate goal is to critically interpret the results in order to identify the best approach to ensure healing in deep wound and to reduce the risk of scaring.

Methods. The study has been carried out according to Helsinki declaration (Ethical Principles for Medical Research Involving Human Subjects). 25 volunteers who underwent surgical reconstruction of different anatomical sites in traumatic wounds, burn and cutaneous neoformation were enrolled. Volunteers were divided into four groups according to the type of surgical treatment they were underwent (split-thickness graft STSG, full-thickness graft, Hyalomatrix dermal scaffold, Integra dermal scaffold).

The instrumental evaluation was carried out on both healthy skin (baseline values or t0) that on different types of skin grafting (t1) according to the group considered.

The High frequency ultrasound scanning was performed by a 22MHz ultrasound device DUB-system (tpm –Taberna pro medicum, Luneburg, DE), 72 µm resolution, 7-8 mm penetration, was used; the B-mode and A-scan were used respectively to acquire skin images and to obtain measurements of skin tissues thickness.

In this study, the 3D imaging of the skin was performed by the digital stripe projection technique using a PRIMOS^{pico} apparatus (GFMesstechnik GmbH, Teltow, Germany). The instrument was used to assess surface roughness parameters of normal and grafted skin.

Results. Results obtained for each of the four groups of volunteers, highlights that the choice of a particular graft and the presence of a dermal substitute influences the fibers organization during the healing process. Ultrasound and 3D visualization techniques demonstrated how modifications in the deeper layers of the skin could impact on its appearance. Furthermore, different autografting techniques led to a dissimilar functional and aesthetic outcomes.

In particular results obtained for the group A using an ultrasound, showed a highly echogenic zone at the level of the dermis which is absent in the zone chooses as a control. According to literature data, this area could be an expression of the last phase of wound healing named *remodeling*. This highly echogenic zone could be responsible for wound retraction in volunteers who had sustained skin lesion which was successfully surgically treated with a split-thickness graft technique.

Wound reconstruction with STSG after use of Hyalomatrix or Integra, leads a different wound recovery if compare to split-thickness skin graft treatment. In the ultrasound images it was possible to visualize a new histological structure known as neodermis.

Conclusions. This work highlighted that high-frequency ultrasound and the 3D image devices, described in this work, can be successfully employed in order to evaluate the skin functional and aesthetic recovery after autografting techniques. Moreover it could be a good starting point to identify the best cutaneous therapy for wound healing improvement.

References

[1] Valencia IC, Falabella AF, Eaglstein WH.,Dermatol Clin., 2000, 18(3):521-32.

[2] Shimizu R, Kishi K.,Plast Surg Int., 2012; 2012:ID 563493.

[3]Myers SR, Partha VN, Soranzo C, Price RD, Navsaria HA, , Tissue Eng., 2007, 13(11):2733-41

[4] Szyman´ ska E., Nowicki A., Mlosek K European Journal of Ultrasound, vol. 12, no. 1, pp. 9–16, 2000.

[5] M. C. T. Bloemen, M. S. van Gerven, M. B. A. van der Wal, P. D. H. M. Verhaegen, and E. Middelkoop, Journal of the American Academy of Dermatology, vol. 64, no. 4, pp. 706–715, 2011.

[6]U. Jacobi, M. Chen, G. Frankowski et al., Skin Research and Technology, vol. 10, no. 4, pp. 207–214, 2004.

IN VITRO BIOCOMPATIBILITY ASSESSMENT OF NOVEL POLYESTER BIOPOLYMERS AND DERIVED NANOPARTICLES

T. Musumeci[1], C. Carbone[1], D. Ramos López[2], J. de Lapuente[2], M. Borràs Suàrez[2], G. Impallomeni[3], A. Ballistreri[1], S. P.P. Guglielmino[4], G. Puglisi[1], R. Pignatello[1]

[1] Department of Drug Sciences, University of Catania, Catania, Italy
[2] UTOX-PCB, Unit of Experimental Toxicology and Ecotoxicology, Parc Científic Barcelona, Barcelona, Spain
[3] Consiglio Nazionale delle Ricerche - ICTP, Catania, Italy
[4] Department of Biological and Enviromental Sciences, University of Messina, Messina, Italy

In these last decades, the field of nanotechnology is experiencing a great development and, as a consequence, the necessity of carrying out studies about the potential hazards and toxicity of nanomaterials, that could threaten their clinical use. In fact, the unique size and surface properties of nanomaterials may be perceived as a "double-edged sword", making them both highly promising therapeutic solutions, able to effectively deliver drug doses at the target tissue and/or in a controlled way, but also potential hazardous entities with tissue penetration properties, possibly deleterious to cell organelles and functions. The rapid development of even more sophisticated nanoparticles leaves their accurate safety evaluation far behind. Several in vitro, in vivo and ex vivo methodologies are available for toxicity assessment (e.g. cytotoxicity, genotoxicity and hemotoxicity), but very few harmonized protocols exist for testing nanomaterials biocompatibility [1].

The aim of the present study is the assessment of the biocompatibility profile of some new biomaterials, which we consider possible candidates for the production of drug delivery systems (DDS) for topical and systemic use [2]. In particular, we tested two series of polymers, belonging to the wide family of aliphatic polyesters. In the first group, two semisynthetic poly(3-hydroxybutyrate-co-ε-capro-lactone) copolymers, namely P1 P(HB-co-72 % CL) and P2 P(HB-co-48 % CL) were studied. The second group consisted of two microbial poly(3-hydroxyalkanoates) (PHAs): P3, obtained from *Pseudomonas oleovorans* cultured on sodium octanoate as carbon source, and P4, obtained from *Pseudomonas aeruginosa* cultured on erucic acid.

The above polymers, and the micro/nanoparticles realized using them, were assessed at different concentrations for hemocompatibility, cyto-, embrio-, and genotoxicity.

A nanoprecipitation method was used to obtain different micro- or nanocarriers. PCS techniques were used for physico-chemical characterization and stability evaluation.

The toxic potential of test samples was evaluated considering different types of toxicity [3, 4]:

- cytotoxicity, evaluated in CaCo2 (Human Caucasian Colon Adenocarcinoma),
- HepG2 (cells derived from hepatocellular carcinoma) and A549 (human lung carcinoma cells) by the viability MTT assay;
- genotoxicity, evaluated in the same cell type by the COMET assay;
- cancerogenicity, evaluated in Balb 3T3 clone A31-1-1 (sensitive to chemical transformation and stable for spontaneous transformation) by Cell transformation assay (CTA);
- embryotoxicity, evaluated in ES-D3 (pluri-potent mouse embryonic cells that can differentiate into cardiomyocytes) by the EST test.

Overall findings confirm that the tested semisynthetic copolymers, that were formed starting from highly biocompatible homopolymers, and the microbial PHAs are safe and well tolerated in different biological models and can therefore be suggested as new biomaterials for producing controlled release or targeted DDS.

Besides, the derived colloidal carriers showed a relatively low toxicological profile, that was correlated to mean size and concentration.

References

[1] Ponti J. et al., Mutagenesis 24, 439 (2009).
[2] Pignatello R. et al, Eur. J. Pharm. Sci. 37, 451 (2009).
[3] Di Guglielmo C. et al., J. Nanosci. Nanotechnol. 12, 1 (2012).
[4] Di Guglielmo C. et al., Reprod. Toxicol. 30, 271 (2010).

A SCREENING OF TECHNOLOGICAL FEATURES AND OCULAR TOLERABILITY OF SURFACTANT AGENTS USED FOR THE PRODUCTION OF LIPID NANOCARRIERS

A. Leonardi[a], S. Cupri[a], C. Bucolo[b], G.L. Romano[b], F. Drago[b], G. Puglisi[a], R. Pignatello[a]

[a] Section of Pharmaceutical Technology, Department of Drug Sciences, &
[b] Section of Pharmacology and Biochemistry, Department of Clinical and Molecular Biomedicine, University of Catania, Catania, Italy

This research work was aimed at evaluating the ocular tolerability of different surfactant agents, commonly used for the production of lipid nanoparticles (SLN and NLC) [1].
In the production of nanostructured systems (lipid and polymeric nanoparticles, nanoemulsions, nanocapsules, etc.), surfactants are generally required as stabilizing agents. Regrettably, ophthalmic application of these nanocarriers needs surfactant removal, because they usually cause irritation of eye tissues. Classic purification processes used to remove surfactants are ultracentrifugation, ultrafiltration, tangential flow filtration (TFF), and dialysis.
Avoiding such purification step after nanocarrier production would offer some advantages, such as time and cost reduction. This would however require to know the maximum surfactant concentration tolerated by the eye structures. Furthermore, by considering the penetration enhancer activity of most surfactants, their residual presence in the formulation would improve the trans-corneal permeation of carried drugs.
In this study, a range of SLN were produced using Dynasan® 114 (glycerin trimyristate) and different surfactant agents: Tween® 80 (polysorbate 80), Kolliphor® P188 (poloxamer 188), SDS (sodium dodecyl sulphate), Kolliphor® HS 15 (macrogol-15-hydroxystearate), Cremophor® A25 (C16~18 fatty alcohol polyoxyethylene ether) and Lipoid® S100 (soy lecithin).
SDS was chosen as a positive control, for its proven ophthalmic irritancy. Surfactant concentrations ranged between 0.05, 0.1, 0.2, and 0.4% (w/v). The Quasi-emulsion Solvent Diffusion method (QESD) was adopted for SLN preparation [2, 3]. The physico-chemical properties (mean particle size and polydispersity index) were determined using photo-correlation spectroscopy (PCS).
While assaying the ability of the tested surfactants to produce homogeneous and stable SLN populations by the QESD method, their ocular tolerability was investigated by a modified Draize test [4, 5]. In particular, to quantify the ocular irritation, the parameters of congestion, swelling and discharge on conjunctiva, corneal opacity and iris hyperemia were evaluated. The stability upon storage of all the produced SLN formulations was also assessed.

Experimental data showed that stable SLN systems, with excellent technological features can be obtained using Dynasan® 114 and Kolliphor® P188. The latter surfactant showed no irritant effect on ocular surface up to a concentration of 0.4% (w/v), whereas Lipoid® S100 and Cremophor® A25 were flawlessly tolerated up to 0.2%.
The results obtained in this work can be used in the future not only for SLN production, but also for polymeric nanoparticles, nanoemulsions and in general nano- or micro-structured systems for ocular application, whose preparation needs the presence of surfactants.

References

[1] Müller R.H. et al., Eur. J. Pharm. Biopharm. 50(1), 161(2000)
[2] Pignatello R. et al., Eur. J. Pharm. Sci. 16(1-2), 53 (2002)
[3] Pignatello R. et al., Biomaterials 23(15), 3247 (2002)
[4] McDonald T.O., Shadduck J.A. In Dermato-toxicology and Pharmacology, Advances in Modern Toxicology; vol. 4, pp. 139-191. Hemisphere, Washington, DC (1977).
[5] Pignatello R. et al., Curr. Drug Deliv. 4, 109 (2007)

SLN-CONTAINING CATIONIC PHOSPHINES AS POTENTIAL NON-VIRAL VECTORS

[1]L. Ravani, [1]E. Esposito, [2]P. Bergamini, [3]M. Drechsler, [1]R. Cortesi,
[1]Dept. of Life Sciences and Biotechnology, University of Ferrara, 44121 Ferrara (Italy)
[2]Dept. of Chemical and Pharmaceutical Sciences University of Ferrara, 44121 Ferrara (Italy)
[3]Macromolecular Chemistry II, University of Bayreuth (Germany)
E-mail: laura.ravani@unife.it

The replacement of defect genes is an intriguing therapeutic system to restore the normal cell function. Cationic systems bind DNA molecules by ionic interaction on their positively charged surface due to the presence of cationic detergents on carrier composition.

Particularly, the purpose of this study was to investigate the potential of solid lipid nanoparticles (SLN) containing new positively charged detergent as nanocarriers for nucleic acids. The cationic character of SLN was obtained by adding as cationic molecules two different long-chain cationic phosphines (CP), namely hexadecyl-PTA iodide (CP16) and octadecyl-PTA iodide (CP18) [1].

CP16 and CP18 have been prepared as iodides by treating in acetone PTA with $C_{16}H_{33}I$ and $C_{18}H_{37}I$, respectively. After production, morphology and dimensions of SLN were characterized by cryo-TEM and photon correlation spectroscopy.

Then, electrophoretic mobility of complexes between CP-SLN and DNA and stability of CP-SLN/pDNA complexes towards fetal calf serum (FCS) contained nucleases were analysed. Finally, the effect of CP-SLN on cell proliferation on cultured human leukemic K562 cells and transfection activity on BHK-2 cells were investigated.

N-alkyl PTA derivatives CP16 and CP18 have been prepared in high yields by reacting 1,3,5-triaza-7-phosphaadamantane (PTA) with the appropriate alkyl iodide. The use of pure tristearin for producing CP-SLN allows the obtaining of stable and homogenous dispersions, free from aggregates. The obtained CP-SLN are characterized by a positive charge on the surface and reproducible dimensions around 220 nm. These nanosystems are able to efficiently bind nucleic acid molecules and to protect DNA from the activity of serum nucleases up to 120 min. Lastly, in vitro experiments demonstrated that CP-SLN exhibit a quite pronounced antiproliferative effect on cultured human K562 erythroleukemic cells and a limited effect as transfecting adjuvant [1].

These data, and particularly the ability of CP-SLN to protect DNA from degradation, encourages further studies aimed at proposing these nanosystems as a potential approach to deliver nucleic acid to cells in living organisms.

References

[1] R. Cortesi et al. Long-chain cationic derivatives of PTA (1,3,5-triaza-7-phosphaadamantane) as new components of potential non-viral vectors. Int J Pharmaceut (2012) 431 (1-2) 176-182

LIPID NANOBUBBLES: PREPARATION AND ACOUSTIC CHARACTERIZATION

Federica Rinaldi[1], Carlotta Marianecci[1], Cinzia Ingallina[2], Angelo Biagioni[3], Andrea Bettucci[3] and Maria Carafa[1]

[1]Department of Chemistry and Drug Technolgies, University of Rome "Sapienza", P.zzle A Moro 5 00185, Rome, Italy

[2]Center for Life Nano Science@Sapienza, Istituto Italiano di Tecnologia,

[3]Department of Basic and Applied Sciences for Engineering, University of Rome "Sapienza", via A. Scarpa 14, 00161, Rome, Italy

Ultrasonography is a widely used imaging technology, non invasive and cost-effective, which is playing a vital role in clinical imaging and diagnosis.
However it shows some limits such as a difficult visualization of vessels smaller than 200 μm in diameter. Commercial ultrasound contrast agents (UCAs), consisting of encapsulated gas microbubbles, enable only a qualitative visualization of the microvascularization for a short period of time since they are rather unstable. In a strategy to develop more stable UCAs, nanobubbles have been prepared with phospholipid coating for a possible use as contrast agents in ultrasound imaging [1].
The aim of this work was the preparation and characterization of lipid nanobubbles (NBs) entrapping a gas, as contrast-enhance ultrasound imaging, and the evaluation of their photothermal signals by means of a photoacoustic sensor in comparison to a clinically approved ultrasound contrast agent consisting of a liquid suspension of micrometric bubbles of SF6 gas (SonoVue® - Bracco Imaging, Milan, Italy). NBs were prepared by the "film" method and the gas (PFC) was loaded by different techniques [2]. NBs were characterized in terms of dimensions, zeta potential and time stability. Photoacoustic is a technique based on the photoacoustic effect, for which light stimulated samples radiate acoustic signals. In this study, a photoacoustic cell is presented for analyzing photothermal signals from nanobubbles/ microbubbles suspended in water or buffer [3].
The obtained results show that vesicular population is characterized by homogenous and monodisperse dimensions, appropriate for drug transport across biological barriers. NBs are stable when stored at 4°C and 25 °C for at least 90 days. Figure 1a reports the frequency spectra of SonoVue® , red curve, compared with the spectrum obtained with distilled water (no bubbles, black curve). Figure 1b reports the comparison between the spectrum of the nanobubble dispersions in Hepes buffer pH 7,4, 10^{-2} M, (red curve) and that of pure Hepes buffer (no bubbles, black curve).
The study of the experimental results highlights the good efficiency of the nanobubble dispersion, in particular the total volume of the gas inside nanobubbles is about 40 percent greater than the gas volume inside SonoVue® microbubbles, regardless of the microbubbles/nanobubbles dimensions.

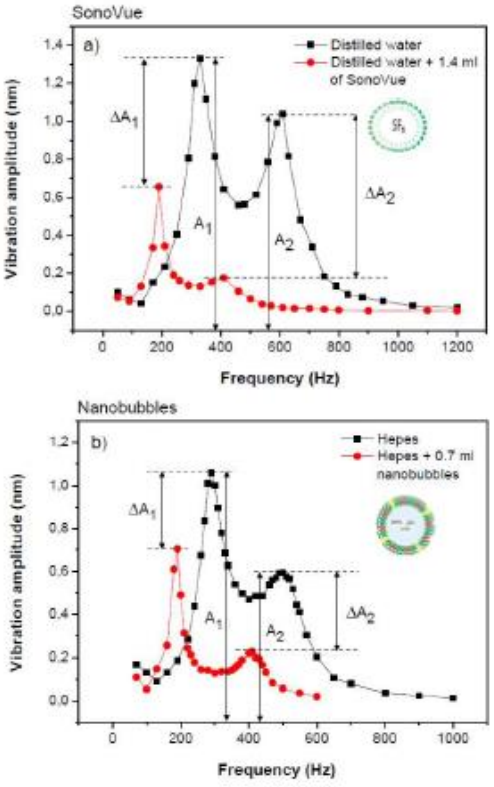

Frequency spectra of SonoVue® (a) and lipid nanobubbles (b).

References

[1] SR Wilson et al. Radiology 257(2010) 24–39
[2] S Ibsen et al. Journal of Controlled Release 155 (2011) 358–366
[3] A Alippi et al. Review of Scientific Instruments 81(2010) 104903.

NANOPARTICLES AS TOOLS FOR CNS CHOLESTEROL DELIVERY IN HUNTINGTON'S DISEASE

B. Ruozi[1], D. Belletti[1], M. Valenza[2], M.A. Vandelli[1], F. Forni[1], E. Cattaneo[2], G. Tosi[1]

[1]*TeFarTI group, Department of Life Sciences, Università di Modena e Reggio Emilia, Via Campi 183, 41100 Modena, Italy;*

[2]*Department of BioSciences and Centre of Stam Cell Research, Università di Milano, Milan, italy*

Alterations in the homeostasis of cholesterol (Chol) are often symptoms of neurodegenerative diseases such as Huntington's disease (HD). The implementation of Chol, with the addition of exogenous Chol, in the CNS appears as a feasible approach in the combined treatment of Huntington's disease [1-3]. Unfortunately, the Chol is not able to cross the blood-brain barrier (BBB). Considering the non-invasive approach, nanocarriers, and particularly polymeric nanoparticles (NPs) could be employed to deliver Chol into the brain. Several in vivo studies demonstrated that modified polymeric nanoparticles prepared starting from a recently approved poly(D,L-lactide-co-glycolide) functionalized with glycopeptides (g7-Nps) cross the BBB and deliver drugs into the CNS [4,5]. By this way, we try to optimize the technological conditions to obtain functionalized polymeric nanoparticles with efficient and stable encapsulation of Chol and able to modulate the drug release in vitro and in vivo into the CNS. The particle size, the polidispersivity (PDI), the particle morphology, the architecture, the surface properties of NPs embedded Chol and the influence of theoretical drug loading on the drug incorporation efficiency were investigated. Then, the NPs embedded Chol or labeled Chol (NBD-Chol) at the optimized polymer/drug ratio (100/1 w/w) were prepared and tested in "multistep" release studies. The ability of NPs to modulate the Chol release was investigated in a) water; b) in vitro cellular studies; c) in vivo studies. A biphasic release of Chol was observed in simulated "in vitro" experiments, with an initial "burst release" (8 % of content during 48h) followed by a plateau and then a second slow release phase (20% during 240h). A gradual/modulate release of drug from NPs was confirmed in "in vitro" cell experiments, by monitoring the fluorescence signal of labeled NBD-Chol embedded and delivered by NPs during transfection in neural stem cells (NS). Finally, to test both the targeting and the ability to release Chol into the CNS, labeled g7-NPs (prepared by using Rhodamine-PLGA during formulation) loaded with NBD-Chol (Rhod-g7-NPs NBD-Chol) were tested in B6CBAF1/J wt mice after ip injection. The release of NBD-Chol from labeled g7-NPs was evaluated by confocal microscopical co-localization studies in different cerebral areas. 12 h after ip administration, NPs (Rhod-PLGA; red signal) co-localized with drug signal (NBD-Chol; green signal). 2 week after ip injection, the two signals only partially co-localized. Only few red spots were present in cerebral areas while an intense and diffuse green points were observed. These data suggested that the translocation of Rhod-g7-NPs NBD-Chol to the brain occurred and that the NBD-Chol is gradually released and diffused into parenchima over time. At the same time NPs were removed from CNS.

Functionality studies are carrying out in HD (R6/2) mice to figure out if and how the delivery of exogenous Chol ameliorate the cerebral function.

Financial Support by the HDF (Hereditary Disease Foundation) NY (USA) is gratefully acknowledged.

References:

1.Valenza, M., et al.: J. Neurosci. 2005, 25: 9932-9939.

2.Valenza, M., et al.: Hum. Mol. Genet. 2007, 16: 2187-2198.

3. Valenza, M., et al.: J. Neurosci. 30, 10844-10850 (2010).

4. Tosi, G., et al.: J. Neural. Transm. 2011, 118: 145-153.

5. Tosi, G., et al.: Nanomedicine 2011, 6: 423-436.

PRODUCTION OF A CAPREOMYCIN SULFATE INHALABLE POWDER BY NANO SPRAY-DRYING

A. Schoubben, S. Giovagnoli, P. Blasi, M. Ricci

Università degli Studi di Perugia, Dipartimento di Chimica e Tecnologia del Farmaco

A 2^3 factorial design was used to individuate the best working conditions to produce inhalable capreomycin sulfate (CS) powders using the Nano spray-dryer B-90 (Büchi Italia Srl). Bacitracin (BAC), a peptide characterized by a similar cyclic structure and high water solubility, was used as model compound to establish the smallest working frame. Stainless steel membrane pore size (A), drying temperature (B) and solution concentration (C) were the chosen parameters. The maximum desirability was intended as the smallest mean volume diameter (d_{mv}) and span, and the highest yield. Other instrument parameters, namely the air flow, the pressure in the drying chamber, the spray rate, were not included in the model and were maintained constant.

Powders were characterized in terms of particle dimensions and morphology (SEM), powder bulk and tap density were also determined to calculate the Hausner ratio (Hr). The best CS powder was characterized for its aerodynamic properties using the glass twin stage impinger [1] and Lactohale LH 200 (DOMO®-Pharma) as carrier.

Varying the three chosen parameters, a high variability was obtained for the yield (18-82%), the d_{mv} (3.12-6.60 µm) and the span (0.91-2.70). The individuated models were highly significant ($p<0.0001$ for the three answers) and the model fitting capability was demonstrated by the non significant lack-of-fit.

Mathematical models evidenced a strong influence of drying temperature and the interactions of drying temperature/BAC concentration, drying temperature/pore size and A^2 on the yield.

The d_{mv} and the span were mainly influenced by BAC concentration, A^2 and its interaction with BAC concentration (A^2C). Moreover, temperature/BAC concentration interaction significantly influenced d_{mv} while only temperature had a significant effect on the span.

The predictivity of the model was successfully validated using four check points. The maximum desirability [2] was obtained spraying a 10 mg/mL BAC solution at 111°C using the 4 µm pore size stainless steel membrane. CS was processed using these conditions and the resulting powder was characterized by a yield of about 82%, a d_{mv} of 3.83 µm and a span of 1.04.

To confirm that the maximum desirability obtained for BAC corresponded to that of CS, a small factorial design was set up to explore the area around the BAC maximum values. This study showed that CS behaved differently and the two compounds do not share the same maximum point. In fact, drug concentration had more influence than temperature on CS characteristics. Applying a desirability function, it has been possible to individuate CS optimized working conditions that are a 6.3 mg/mL CS solution, 102°C drying temperature and the 4 µm pore size stainless steel membrane. Using these conditions, CS powder was characterized by a yield about 71%, a d_{mv} of 3.25 µm and a span of 0.95. SEM showed spherical particles with a smooth surface and dimensions corresponding to those determined using the "single particle optical sensing" technique [3]. The starting CS powder and the nano spray-dried powder have a Hr of 1.0997 and 1.2957, respectively. CS aerodynamic diameter, calculated considering perfectly spherical particles and a tap density of 0.369 g/mL, was of 1.95 µm. Since CS flow properties were altered by the reduced dimensions, lactose was used as carrier to evaluate CS respirable fraction that was around 27% (~ 14% without lactose) while the emitted dose was of 87%.

Thanks to the factorial design and to the use of a model compound, it was possible to produce CS powders with the appropriate size for inhalation and a good yield, performing a reduced number of experiments. Lactose, used as carrier, consented to improve CS aerodynamic properties.

References

[1] European Farmacopea VI Ed, 2008. pp. 287-288.
[2] Derringer G and Suich R, J. Qual. Technol. 12, 214 (1980).
[3] Nicoli DF et al, Am. Lab. 24, 39 (1992).

HOT-MELT EXTRUSION AND INJECTION MOLDING AS ALTERNATIVE TECHNIQUES FOR THE MANUFACTURING OF IR DOSAGE FORMS

A. MELOCCHI, L. ZEMA, G. LORETI, F. CASATI, A. MARONI, A. GAZZANIGA

Università degli Studi di Milano, Dipartimento di Scienze Farmaceutiche, Sezione di Tecnologia e Legislazione Farmaceutiche "Maria Edvige Sangalli", 20133 Milano, Italia

Introduction

The interest in the potential application of the continuous manufacturing approach to the pharmaceutical field has been growing in the last few years [1-3]. Continuous manufacturing consists in producing or processing, without interruption, materials that are generally maintained continuously in motion while undergoing chemical reactions or mechanical/heating treatments. When applied to the manufacturing of drug products, this approach could reduce development time and costs by *i)* overcoming the stopping, re-configuration and testing between batches as well as the need for scaling up, *ii)* improving the process efficiency (time-monitoring of the process, quality of products) and production space exploitation. Hot-melt extrusion (HME) and injection molding (IM) represent the main techniques that fulfil the needs of the continuous approach for the manufacturing of dosage forms [4]. However, they are not much commonly used in the pharmaceutical industry, and in this area they are especially employed for the development of drug delivery systems [5-7]. Based on these premises, a research project was started to assess the potential of HME and IM for the manufacturing of immediate-release (IR) dosage forms and particularly tablets as they are the blockbuster in the field. Indeed, these are manufacturing techniques mentioned in the pharmacopoeial monograph relevant to tablets (Eur. Pharm. 7th ed.) while no systematic evaluation of their feasibility has been undertaken so far. In the present work, a screening of polymeric carriers and functional aids has been carried out along with the identification/ selection of parameters and procedures for the characterization of extruded/molded tablets.

Experimentals

Materials Hydroxypropyl cellulose (**HPC**; Nisso SSL, J); hydroxypropyl methyl cellulose (**HPMC**; Methocel E5, Colorcon, US); polyvinyl alcohol (**PVA**; Gohsenol, Nippon Goshei, J); polyvinyl alcohol-polyethylene glycol graft copolymer (**KIR**; Kollicoat® IR, BASF, D); polyvinyl caprolactam-polyvinyl acetate-polyethylene glycol graft co-polymer (Soluplus®, BASF, D); corn starch (Ingredion, US); sodium starch glycolates (**EXP,** Explotab®; **EXP$_{CLV}$**, Explotab® CLV; **VIV**, Vivastar®; JRS Pharma, D); vinylpyrrolidone-vinyl acetate copolymer (**KVA**; Kollidon® VA 64, BASF, D); deionized water (**W**); glycerol (**GLY**; Pharmagel, I), polyethylene glycols (**PEG** 400, 1500, 6000 and 8000; (Clariant Masterbatches, I); talc (Carlo Erba, I); croscaramellose sodium (AcdiSol®, FMC BioPolymer, US); sodium chloride (**NaCl**, Carlo Erba, I); sodium hydrogen carbonate (**$NaHCO_3$**, Carlo Erba, I); calcium carbonate (**$CaCO_3$**, Carlo Erba, I); citric acid (Carlo Erba, I); tartaric acid (Carlo Erba, I); furosemide (Metapharmaceutical, E).

Methods Polymers, stored 24 h in oven at 40 °C, were mixed/granulated in a mortar with plasticizers (% by weight calculated with respect to the dry polymer); functional adjuvants and/or drugs were subsequently added and mixed in mortar (% by weight on the blend).

TABLET MANUFACTURING: HME was carried out by a single-screw extruder (Extrusiograph 19/25D, Brabender, D) equipped with a rod-shaped die (ø 8 mm). Extruded products were cut into tablets (h 4 mm) by means of a bench-top saw. IM was performed by a bench-top micromolding machine (BabyPlast 6/10P, Cronoplast S.L.; Rambaldi S.r.l., Italy) equipped with a disk-shaped (ø 30 mm and h 1 mm) or cylindrical (ø 8 mm and h 4 mm) mold. As far as starch and starch derivatives are concerned, they were preliminarily extruded to achieve thermoplastic properties.

DISINTEGRATION/DISSOLUTION ABILITY OF TABLETS: **Mass loss by dissolution** (apparatus 2 USP35, Dissolution System Distek Inc. 2000, USA; 1000 mL deionized water, 37 ± 0.5 °C, 100 rpm): in order to withdraw and weigh samples during the test, these were inserted into a polyethylene net (2 mm mesh). **Mass loss by disintegration** (adapted six-position disintegration apparatus USP35; 800 mL deionized water, 37 ± 0.5 °C, 31 cycles/min): each basket-rack was filled with one sample. At established time points samples were withdrawn and dried in a oven (40 °C) to constant weight. **Drug dissolution test** (apparatus 2 USP35, Dissolution System Distek Inc. 2000, USA; 1000 mL deionized water, 37 ± 0.5 °C, 100 rpm): fluid samples were withdrawn at fixed time points and assayed spectrophotometrically (277 nm).

Results and discussion

In order to perform HME and/or IM processes, tablet-forming agents (*i.e.* fillers) were selected for screening among thermoplastic polymers. Besides the potential ability to be processed into tablets, such polymeric carriers were expected to prompt/enable drug liberation (disintegration/dissolution), thus limiting the need for any type of adjuvant (simplification of the formulation). In this respect, polyethylene glycols, which have already been proposed for the manufacturing of tablets by IM, may represent a critical material [8]. In fact, they are characterized by very low melting points and viscosities so that they could not be processed without a solid component dispersed, giving rise to poorly physically stable products. Soluble polymers, traditionally employed for the preparation of solid dispersions by HME or used for cosmetic-coating of solid dosage forms, and tablet-fillers of common use, such as starch, were therefore selected. In addition, starch-derived superdisintegrants (*i.e.* sodium starch glycolate) were considered as they could show, like starch, a thermoplastic behavior under specific conditions (*i.e.* presence of plasticizers and shear stress) and maintain a potential as disintegrants [9].

For each of the selected polymers, the feasibility of HME and IM processing and the need for technological adjuvants (*e.g.* plasticizers) were explored. Moreover, the influence of functional adjuvants, *i.e.* components added to the formulation in order to improve the disintegration/dissolution ability of the polymeric

carrier (*e.g.* soluble or insoluble fillers, disintegrants, effervescent excipients) was evaluated.
Molded disks of 1 mm thickness were prepared as screening tools for a preliminarily evaluation of the selected materials in terms of processability and mass loss behavior under dissolution testing conditions. Afterwards, tablets were prepared by IM and HME, and their ability to disintegrate/dissolve was assessed by means of a modified disintegration test. In both cases, the times to 10, 50 and 80 % of mass loss were calculated ($t_{10\%}$, $t_{50\%}$ and $t_{80\%}$, respectively). By way of example, data are reported relevant to the screening of polymers (Table I) and the influence of functional adjuvants on mass loss from IM tablets based on the most promising polymeric materials, *i.e.* HPC and EXP_{CLV} (Table II). Moreover, dissolution profiles of tablets containing a poorly-soluble model drug are shown in Fig. 2.

Table I: processability by IM and data of $t_{10\%}$ mass loss by dissolution (CV< 5 %) relevant to screening items

polymer	plasticizer (% w/w)	processability	$t_{10\%}$ (min)
HPC	PEG 1500 (10%)	+	2.57
HPMC	PEG 400 (50%)	-/+	4.09
KIR	GLY (15%)	+	4.34
KVA	PEG 1500 (10%)	-	-
PVA	GLY (20%)	+	3.79
Soluplus	PEG 1500 (15%)	-/+	8.23
Starch	W (15%) + GLY (10%)	-/+	10.12
EXP	W (20%) + GLY (20%)	-/+	3.42
EXP_{CLV}		-/+	2.47
VIV		-/+	3.28

"-" incomplete disks; "-/+" complete disks not automatically ejected; "+" complete disks automatically ejected.

Most of the materials tested exhibited the ability to be processed with no need for technological aids except for a plasticizer.
HPC and EXP_{CLV} were identified as promising tablet-forming agents showing a different disintegration/ dissolution behavior (Fig. 1).

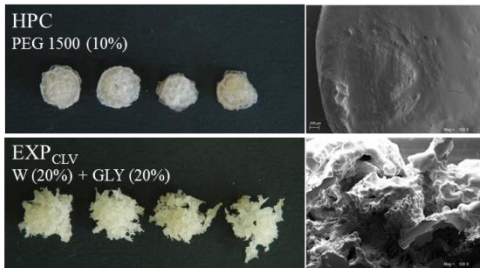

Fig. 1: photographs of dried HPC and EXP_{CLV} tablets withdrawn at successive time-points from the dissolution medium and relevant SEM photomicrographs (5 min)

- HPC acts as a soluble filler and the relevant tablet shows a progressive decrease in volume, whereas EXP_{CLV} exhibited an intrinsic ability to disintegrate thus leading to an increase in the tablet area exposed to the aqueous fluids. Accordingly, HPC-based tablets containing a poorly-soluble model drug displayed a very slow dissolution, whereas over 30 % of drug was dissolved within 30 min in the case of tablets based on EXP_{CLV} as such (Fig. 2).

- The disintegration/dissolution performance of tablets was generally improved by the addition of functional adjuvants, especially in the case of disintegrants and effervescent excipients that were demonstrated to also maintain their properties after being processed by IM. Accordingly, the dissolution performance of the model drug was largely improved (Fig. 2).

Table II: data of $t_{10\%}$ and $t_{80\%}$ mass loss by disintegration (CV < 5 or 15 %, respectively) relevant to HPC- and EXP_{CLV}-based tablets containing functional adjuvants

	HPC PEG 1500 (10%)		EXP_{CLV} W (20%) + GLY (20%)	
Functional adjuvant (% w/w)	$t_{10\%}$	$t_{80\%}$	$t_{10\%}$	$t_{80\%}$
-	18.8	> 90	5.26	49.09
30 % AcdiSol	9.33	88.27	1.00	25.49
50 % AcdiSol	6.48	61.79	6.48	54.62
30 % EXP_{CLV}	4.14	60.79	1.94	36.04
50 % EXP_{CLV}	10.92	> 90	-	-
30 % $NaHCO_3$	3.46	50.60	7.66	81.28
30 % $NaHCO_3$ (52.83 %) + tartaric acid (47.17 %)	1.48	32.82	4.02	55.26
30 % $NaHCO_3$ (52.27 %) + citric acid (36.36 %) + $CaCO_3$ (11.36 %)	1.81	46.87	1.68	41.83
30 % Talc	4.43	65.18	1.21	44.64
30 % NaCl	5.88	43.28	1.85	65.11
30 % KIR	2.01	34.59	4.85	40.05

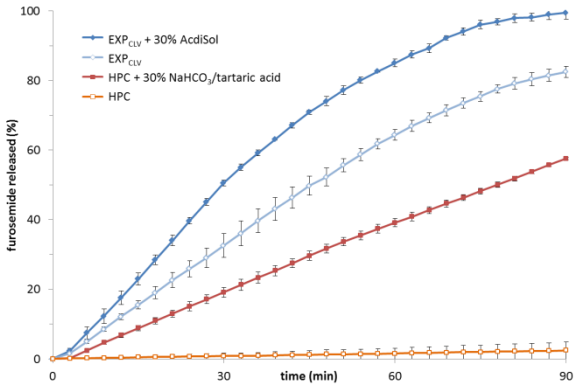

Fig. 2: dissolution profiles of IM tablets containing a poorly soluble drug

Conclusion

The possibility of exploiting HME and IM techniques for the continuous manufacturing of tablets was preliminarily assessed and promising results were obtained in terms of viable formulation strategies.

References

[1] Plumb K., Chem. Eng. Res. Des., 83, 730-738 (2005).
[2] Vervaet C. et al., Chem. Eng. Sci., 60, 3949-3957 (2005).
[3] Schaber S. D. et.al., Ind. Eng. Chem. Res., 50, 10083-10092 (2011).
[4] Ghebre-Sellassie I. Ed., Pharmaceutical extrusion technology, Marcell Dekker Inc. (2003).
[5] Zema L. et al., J. Control. Rel., 159, 324-331 (2012).
[6] Gazzaniga A. et al., AAPS PharmSciTech., 12, 295-303 (2011).
[7] Zema L. et al., Int. J. Pharm., 440, 264-272 (2013).
[8] Cuff G., Raouf F., Pharm. Technol. Eur., 22, 96-106 (1998).
[9] Zema L. et al., Int. J. Pharm., 440, 264-272 (2013).

FREEZE-DRYING OF INSULIN-LOADED SOLID LIPID NANOPARTICLES: FROM MORPHOLOGY TO PROTEIN STRUCTURE

Sandra Soares[1], Ana Costa[1], Pedro Fonte[1,2], Bruno Sarmento[1,3]

[1]CESPU, Instituto de Investigação e Formação Avançada em Ciências e Tecnologias da Saúde, Gandra-PRD, Portugal
[2]REQUIMTE, Department of Chemistry, Faculty of Pharmacy, University of Porto, Porto, Portugal
[3]INEB – Instituto de Engenharia Biomédica, University of Porto, Porto, Portugal

Introduction

Solid lipid nanoparticles (SLN) have been successfully used to protect proteins from degradation and deliver it in a sustained manner. In addition, the incorporation of proteins into SLN may enhance their bioavailability by facilitating its transmucosal transport. Biocompatibility and biodegradability are major advantages of these systems since their matrix is made by lipids GRAS (Generally Recognized As Safe). Several research groups had successfully encapsulated insulin into SLN, however the maintenance of protein integrity after processing methods remains unclear, and even less is known concerning the long-term stability and shelf-life behaviour of insulin structure when encapsulated into nanoparticles formulations.
Freeze-drying is the most common technique to preserve biopharmaceuticals for extended periods of shelf-lives, however, it is a stress source itself, which can damage proteins or destabilize the formulation. To avoid this, several sugars are being used as cryoprotectants since they shown ability to preserve lipid carrier properties and native structure of proteins after freeze-drying.

Goal of the work

The aim of this work was to assess the secondary structure of insulin after encapsulation into SLN and after freeze-drying with different cryoprotectants. Additionally, insulin-loaded SLN (Ins-SLN) stability over time was also assessed in a 6 months stability study following the ICH guidelines.

Experimentals

SLN (Witepsol E85/PVA 1%) were prepared by a modified solvent emulsification-evaporation w/o/w double emulsion technique [1]. SLN formulation was divided into two groups, one intended for freeze-drying and another to keep in suspension form.
SLN were freeze-dried using no cryoprotectant; and fructose, glucose and sorbitol as cryoprotectants at 10% (w/w). All samples were frozen at −80ºC for 6 h, transferred to a freeze-dryer maintained at 0.09 mbar, and at a condenser surface temperature of −60 ± 5◦C during 72 h.
Samples were distributed for three different storage conditions of temperature/relative humidity (RH) at: 4 ± 2◦C/60 ± 5% RH, 25 ± 2◦C/60 ± 5% RH and 40 ± 2◦C/75 ± 5%RH. Samples were analyzed after production and freeze-drying (t0), and after 1, 3 and 6 months (t1, t3 and t6, respectively) of storage in terms of particle size and zeta potential and were visualized by TEM and SEM. Ins-SLN stability was monitored by FTIR to evaluate insulin secondary structure during storage time, using a double subtraction procedure [2]. The quantitative comparison with native insulin was assessed using the spectral correlation coefficient (SCC) and area of overlap (AO) algorithms [1]. All samples were run in triplicate.

Results and discussion

Ins-SLN were produced with a mean diameter of 400 ± 47 nm, a PdI equal to 0.17 ± 0.05 and a zeta potential of −13.3 ± 0.4 mV, parameters which maintained after freeze-drying with no cryoprotectant added (Figure 1). The AE of Ins-SLN was 84.8 ± 0.05%.

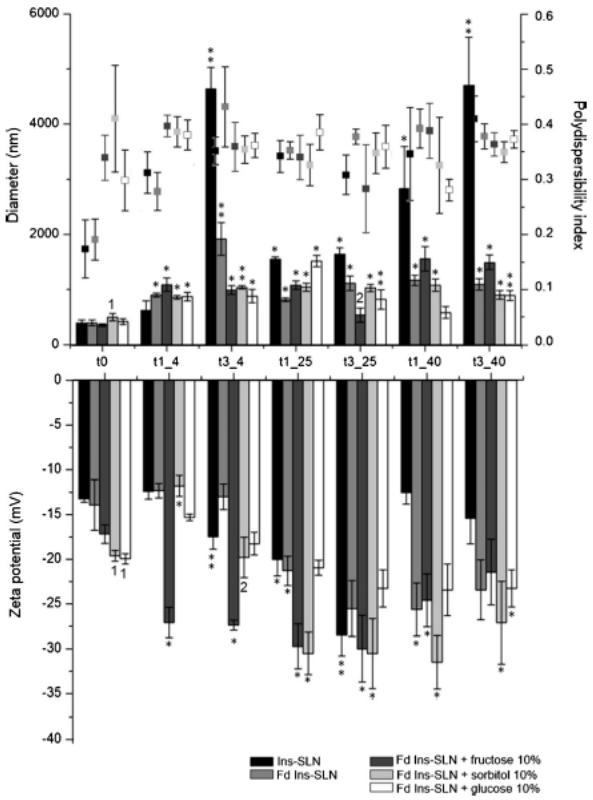

Figure 1. Diameter (top bars), polydispersity index (square symbols) and zeta potential (bottom bars) characterization of Ins-SLN formulations. Results are significantlydifferent from corresponding t0 or, t0 and t1 when marked with asterisk or double asterisk, respectively. Results marked with (1) mean that are significantly different from the results of Ins-SLN in suspension and after freeze-drying at t0; (2) do not differ from corresponding t0 result but differ from t1.

The obtained results shows that cryoprotectant-added formulations did not reveal superior quality comparatively to sugar-free formulations in terms of particle size and aggregation after rehydration. This occurs because cryoprotectants definitely change the physical properties of the SLN formulations, which lead to unpredictable behaviors upon a non-optimized freeze-drying process.

Over 6 months, Ins-SLN with cryoprotectant showed no significant alterations in nanoparticles shape, once that the spherical shape is maintained, which is a good indicator of the lipid structural stability (Figure 2).

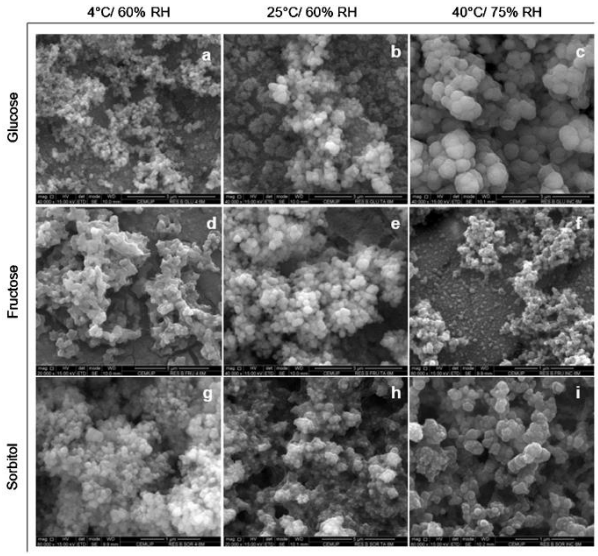

Figure 2. SEM images of freeze-dried Ins-SLN formulations with cryoprotectant added, stored at different conditions after 6 months. Scale bar: (a)–(c), and (e) 3 µm; (d) and (h) 5 µm; (f), (g) and (i) 1 µm.

Figure 3 shows the AO and SCC values of all the tested samples, which represent a degree of similarity with native insulin structure. Generally, those values revealed some variability and, as expected, SLN formulations in liquid state were the most affected, since insulin is vulnerable to the hydrolytic action of water, suffering earlier denaturation. Ins-SLN AO after production was 92.5 ± 0.6%, diminishing to 74.2 ± 0.5% (at 4◦C/60%RH) and to 63.7 ± 1.2% (at 25◦C/60%RH) after 6 months. The worse drop went to 51.3 ± 3.9% in 3 months at 40◦C/75%RH.

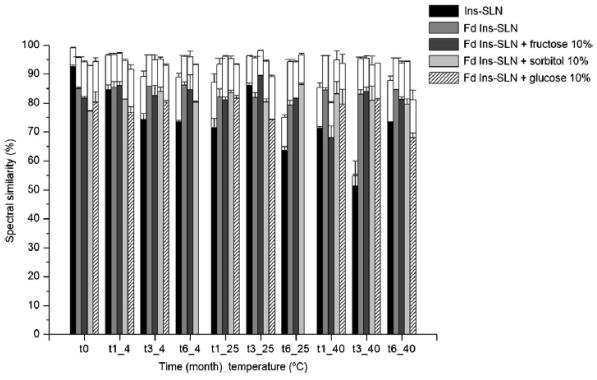

Figure 3. Area overlap (coloured bars) vs correlation coeficient (white bars) percentages obtained from the area-normalised second-derivative amide I spectra of Ins-SLN in suspension and, freeze-dried without cryoprotectant or with fructose, sorbitol and glucose at 10% (w/w), comparatively to native insulin.

In freeze-dried form, Ins-SLN without cryoprotectant was the formulation with higher spectral similarity percentages (84.9 ± 0.4 of AO, and 95.7 ± 0.2% of SCC) after freeze-drying (t0) and with the smaller variability over time and among storage conditions, reaching identical spectral similarity values after 6 months even at 40◦C/75%RH (Figures 3 and 4). Overall, Ins-SLN formulations without cryoprotectants showed the greatest stability among all formulations tested.

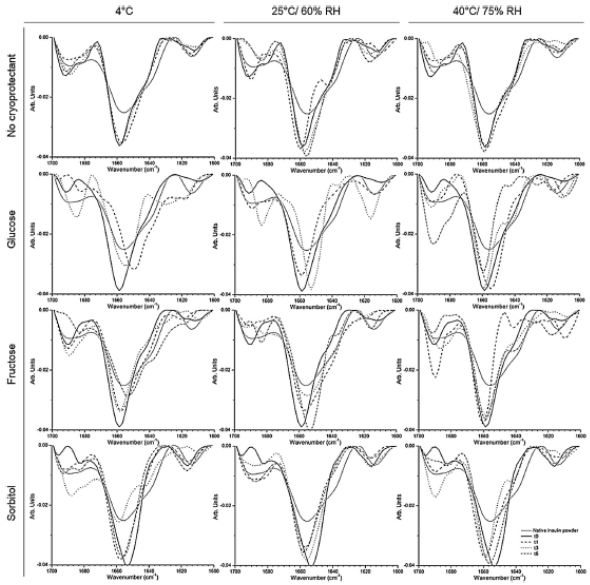

Figure 4. Comparison of the area-normalized second-derivative amide I spectra of native insulin and freeze-dried Ins-SLN formulations.

Conclusion

Through a non-optimized freeze-drying process, SLN revealed its ability to retain insulin structure after freeze-drying and even under harsh conditions of storage during six months of shelf-life. Despite some nanoparticle aggregation occurred during storage, freeze-drying process improved the long-term physical-chemical stability of Ins-SLN. Adding cryoprotectants did not offer superior stability, mostly because insulin was successfully encapsulated into SLN, without subsequent direct contact with cryoprotectants. The non-optimized combination of cryoprotectant and freeze-drying process resulted in alterations of the SLN physicochemical properties, leading to lack of protein structure protection. Further development with multivariable experimental design will help to find the process parameters settings that best fit with the desired product quality attributes regarding protein and nanoparticle stability.

References

1. Soares, S., et al., *Effect of freeze-drying, cryoprotectants and storage conditions on the stability of secondary structure of insulin-loaded solid lipid nanoparticles.* International Journal of Pharmaceutics, 2013. **456**(2): p. 370-381.
2. Sarmento, B., et al., *Probing insulin's secondary structure after entrapment into alginate/chitosan nanoparticles.* European Journal of Pharmaceutics and Biopharmaceutics, 2007. **65**(1): p. 10-17.

TOWARDS THE CHARACTERIZATION OF AN IN VITRO TRIPLE CO-CULTURE INTESTINE CELL MODEL FOR PERMEABILITY STUDIES

Francisca Araújo[1,2], Filipa Antunes[3], Fernanda Andrade[3], Domingos. Ferreira[3], **Bruno Sarmento**[1,2*]

[1] INEB – Instituto Engenharia Biomédica, University of Porto
[2] Health Sciences Research Center (CICS), Department of Pharmaceutical Sciences, Instituto Superior de Ciências da Saúde-Norte, Gandra, Portugal
[3] Department of Pharmaceutical Technology, Faculty of Pharmacy, University of Porto, Portugal
*bruno.sarmento@ineb.up.pt

Introduction

In vitro cell culture models for studying oral drug absorption during early stages of drug development have become a useful tool in drug discovery and development, with respect to substances throughput and reproducibility. Numerous *in vitro* methods have been used in the drug selection process for assessing the intestinal absorption potential of drug candidates. Despite the absence of many important features, with major influence in the drug absorption mechanism, Caco-2 cell model has been undoubtedly, the gold standard and the most accepted *in vitro* cell model to study the intestinal permeability [1,2].

Goal of the work

The aim of this study was to establish and characterized an *in vitro* triple co-culture based on human colon carcinoma Caco-2 cellular model, in order to design a model that more accurately mimics the small intestinal epithelial layer. This model, besides enterocytes, also comprises mucus-producing HT29-MTX cells and Raji B cells. With this model was intended to evaluate the seeding ratio between Caco-2 and HT29-MTX cells to achieve physiological proportions after cells maturation and differentiation in culture and the formation of M-cells phenotype from enterocytes. Furthermore, the permeability of chitosan-based nanoparticles containing therapeutic proteins was evaluated. Simultaneously, the new *in vitro* cellular model was also used to track possible protein transport mechanisms through the intestinal membrane.

Experimentals

Inverted and normal oriented *in vitro* models of triple co-culture Caco-2:HT29-MTX:Raji B were assessed. On the normal oriented model, Caco-2 and HT29-MTX cells were seeded into Transwell® inserts and Raji B cells added to the basolateral chamber of 14-day-old Caco-2:HT29-MTX co-culture. Cultures were maintained for 4–6 days. On the inverted model Caco-2 and HT29-MTX cells were seeded on the lower face of Transwell® inserts and cultured overnight. After fully differentiated, Raji B cells were added to the apical compartment, following an adapted protocol previously reported [3]. Transepithelial Electrical Resistance (TEER) values of the cell membranes were monitored throughout the entire experiment time. Monocultures of Caco-2 cells were used as controls.
To confirm the initial seeding proportions between the cells in the co-cultures after the 21 days in culture, flow cytometry experiments were performed using EGFP transfected Caco-2 cells. To see morphological differences between different cell types, the alcian blue histochemical method was made in order to label the mucus and immunocytochemical techniques were executed to identify M-cells.
Insulin transport, both in solution and encapsulated into biodegradable dextran sulfate/chitosan nanoparticles [4] was monitored by HPLC from apical to basolateral chambers.

Results and discussion

All the three cell lines maintained their function when cultured together with each other. The seeding ratio of 90:10 between Caco-2 and HT29-MTX showed to be the best to achieve physiological proportions after cells maturation and differentiation in culture (Figure 1).

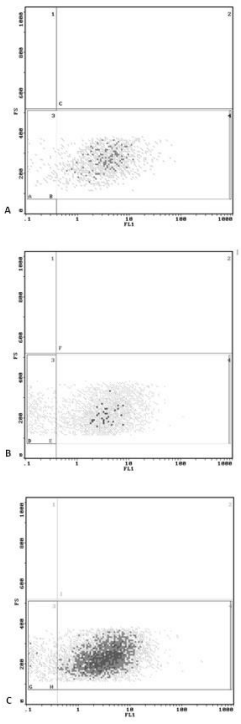

Figure 1: Caco-2:HT29-MTX cells proportions after 21 days in culture. Initial seeding rate of 90:10 proportion resulted in a culture with 95% ± 0.5 of Caco-2 cells (A); the initial seeding rate of 80:20 proportion resulted in a culture with 94% ± 1.6 of Caco-2 cells (B) and the seeding rate proportion of 70:30 resulted in a culture with 90% ± 0.7 of Caco-2 cells (n=5, mean ± SD).

The formation of M-cells phenotype from enterocytes was identified for the first time in a co-culture system comprising Caco-2 and HT29-MTX (Figure 2). Insulin absorption from insulin loaded dextran sulfate/chitosan nanoparticles was higher on normal oriented cell cultures, as well as the TEER values on the same (Figure 3 and 4). For both, normal and inverted models, insulin absorption was higher when HT29-MTX cells were introduced on the co-culture model.

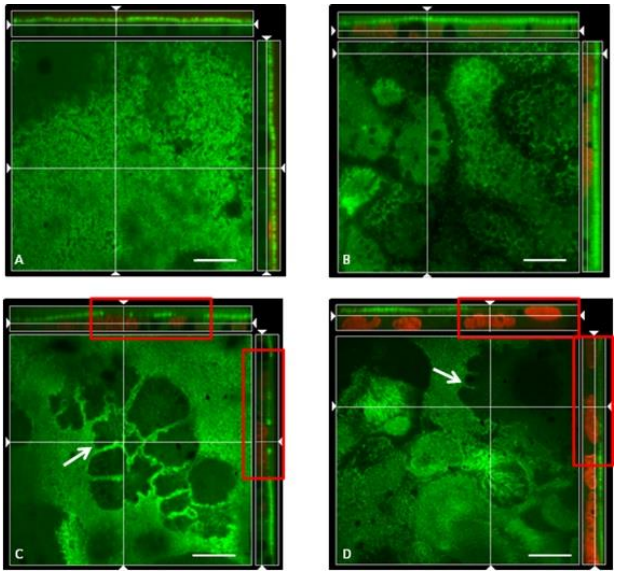

Figure 2: M-cell phenotype induction by Raji B cells. A continuous actin label can be seen in Caco-2 monocultures (A) and in Caco-2:HT29-MTX dual co-culture (B), proving the presence of microvilli in the surface of the cells. In Caco-2:Raji B dual co-culture (C) and Caco-2:HT29-MTX:Raji B triple co-culture (D) the labeling is discontinuous in some areas (arrows) filled with nucleus (squares) showing the absence of microvilli in the cells. Actin was labeled with Alexa Fluor® 488 Phalloidin presenting a green color and nuclei labeled with IP presenting a red color. Bar = 5µm.

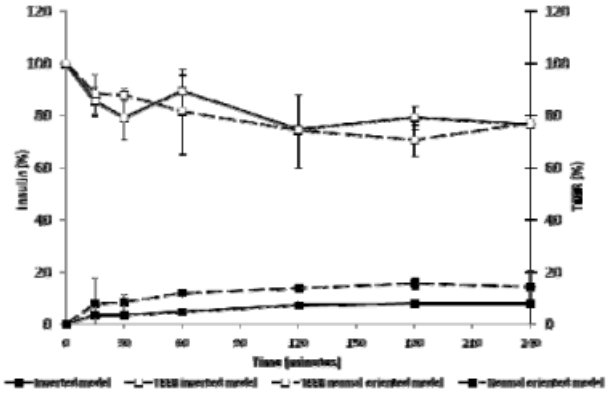

Figure 3: Cumulative insulin transport and TEER measurements from insulin loaded dextran sulfate/chitosan nanoparticles across both normal oriented and inverted co-culture models Caco-2/Raji B.

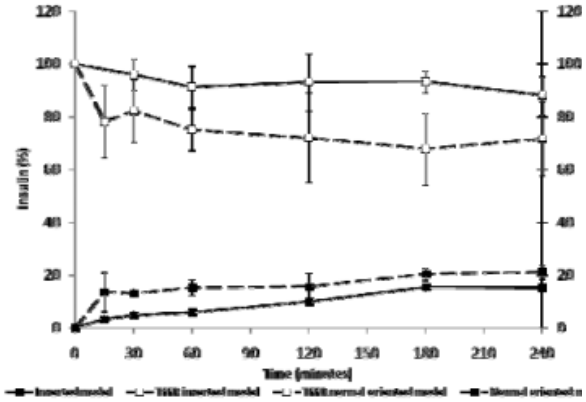

Figure 4: Cumulative insulin transport and TEER measurements from insulin loaded dextran sulfate/chitosan nanoparticles across both normal oriented and inverted triple co-culture models Caco-2:HT29-MTX:Raji B.

Dextran sulfate/chitosan nanoparticles enhance the insulin absorption through the cellular models used, compared to insulin solution. The mucoadhesive and absorption-enhancing properties of chitosan may be fundamental to the transient opening of tight junctions connecting epithelial cells, thus endorsing insulin diffusion through the epithelium, promoting insulin absorption [5]. The staining with Alcian Blue dye highlighted the presence of mucus on the co-culture models containing HT29-MTX cells, not present when this cell line is absent (results not shown).

Conclusion

The normal triple co-culture model presented in the herein work is a good and reliable alternative to the *in vitro* methods already existents for the study of drugs permeability and it may correlate *in vivo* intestinal absorption. Also, dextran sulfate/chitosan nanoparticles enhance the insulin absorption as quantified in this cellular model.

References

1. F. Araújo, B. Sarmento (2013). Towards the characterization of an *in vitro* triple co-culture intestine cell model for permeability studies. International Journal of Pharamceutics. *In press*.
2. F. Antunes, F. Andrade, F. Araújo, D. Ferreira, B. Sarmento (2013). Establishment of a triple co-culture *in vitro* cell models to study intestinal absorption of peptide drugs. European Journal of Pharmaceutical Sciences, 83(3), 427-35.
3. A. des Rieux, V. Fievez, I. Théate, J. Mast, V. Préat, Y-J. Schneider (2007). An improved *in vitro* model of human intestinal follicle-associated epithelium to study nanoparticle transport by M cells. European Journal of Pharmaceutical Sciences, 30. 380-391.
4. B. Sarmento, A. Ribeiro, F. Veiga, D. Ferreira, R. Neufeld (2007) Oral bioavailability of insulin contained in polysaccharide nanoparticles, Biomacromolecules , 8. 3054-3060.
5. P. Fonte, T, Nogueira, C. Gehm, D. Ferreira, B. Sarmento (2011), Chitosan-coated solid lipid nanoparticles enhance the oral absorption of insulin, Drug Delivery and Translational Research , 1, 299-308.

ORAL DELIVERY PLATFORMS IN THE FORM OF "FUNCTIONAL CONTAINERS" PREPARED BY INJECTION MOLDING

L. ZEMA, G. LORETI, A. MELOCCHI, F. CASATI, E. MACCHI, A. GAZZANIGA

Università degli Studi di Milano, Dipartimento di Scienze Farmaceutiche,
Sezione di Tecnologia e Legislazione Farmaceutiche "Maria Edvige Sangalli", 20133 Milano, Italia

Introduction

Drug delivery systems are aimed at improving the therapeutic performance of drug molecules, limiting their adverse reactions or enhancing patient compliance. As far as the oral route is concerned, many formulation strategies have been proposed to increase the bioavailability or modify the release of drugs in terms of rate, time and/or site. A large number of such systems are conceived in the form of a drug-containing core coated with a functional barrier based on polymeric materials with peculiar properties such as pH-dependent solubility, enzyme degradability, slow interaction with aqueous fluids (glassy-rubbery transition and consequent erosion/dissolution), bioadhesion or permeability. The traditional *reservoir*-design could be improved if the drug core and the functional coat could be dealt with as independent items, *i.e.* a "functional container" and the contents formulation. One of the most commonly used techniques for the preparation of polymeric objects is injection molding (IM), which recently demonstrated to hold promises for the pharmaceutical field in terms of versatility (not only shape and dimensions of the container but also effectiveness of the locking system), patentability and scalability [1].

Goal of the work

The aim of the present work is the evaluation of the feasibility of release platforms in the form of enteric-soluble, pulsatile/delayed or prolonged-delivery "containers". They should be composed of separately-manufactured parts that could be assembled in a subsequent production stage (capsular containers) after being filled with various drug-formulations through well-established filling procedures. The performance of such devices should depend on their composition and design features (morphology and thickness of the shell) only, in spite of differing characteristics of the conveyed drug and/or formulation, which would offer major advantages in terms of time and costs required for development.

Experimentals

Materials - hydroxypropyl cellulose (HPC, Klucel® EF and LF, Ashland, US); hydroxypropyl methyl cellulose acetate succinate (HPMCAS, AQUOT-LG®; Shin-Etsu, J); ethylcellulose (EC, Ethocel® 100 std; Dow, US); polyethylene glycol (PEG 1500; Clariant Masterbatches, I), triethyl citrate (TEC; Aldrich, US); sodium starch glycolate (Explotab® CLV; JRS, Rettenmaier Italia, I); acetaminophen (AAP, C.F.M., I).

Methods - molded products were obtained by means of a bench-top microinjection molding press (BabyPlast 6/10P, Chronoplast, Rambaldi, I) equipped with different molds for the manufacturing of capsular containers of different size and shape (Fig. 1). Molded items were characterized by weight, dimensions, mechanical resistance and dissolution/release properties (Dissolution System 2100B, Distek, US). Preliminary *in vivo* studies were performed on healthy volunteers collecting saliva samples analyzed by a previously set up gradient RP HPLC (Waters Co., US) method.

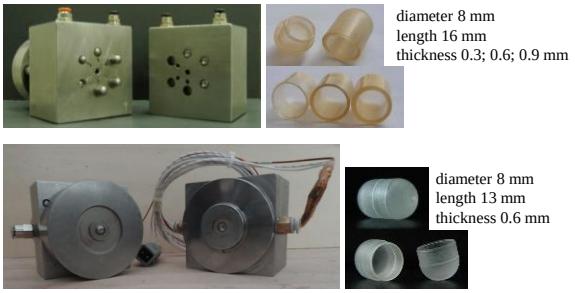

Figure 1 pictures of molds and examples of molded items

Results and discussion

Pulsatile/delayed-delivery container. A hydrophylic swellable polymer with thermoplastic properties needed to be selected: HPC. In order to achieve an acceptable balance between processability and mechanical properties of the molded units, a plasticized formulation was developed containing 10 % w/w of PEG 1500. The slow interaction with aqueous fluids of the polymeric shell (formation of a gel boundary and subsequent dissolution/erosion) was demonstrated to impart a lag phase to the release of capsule contents (Fig. 2).

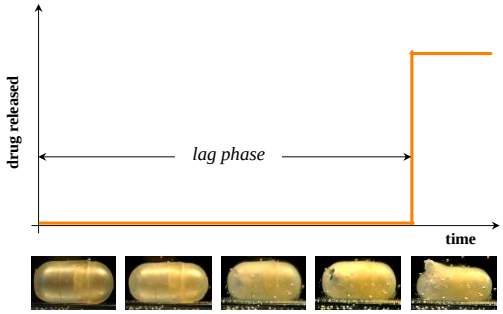

Figure 2 theoretical release profile of the HPC capsules

Data relevant to *in vitro* and *in vivo* studies are reported in Fig. 3; the duration of the delay can be modulated changing the shell composition (viscosity grade of

HPC) and thickness. *In vivo* lag times up to 3 h were achieved.

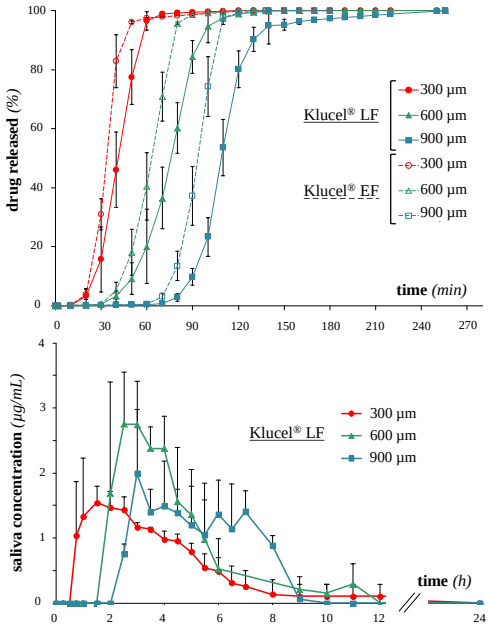

Figure 3 *in vitro* (top) and *in vivo* (bottom) performance of HPC-based pulsatile/delayed delivery capsular containers with different shell composition and thickness [2,3]

Gastroresistant container. HPMCAS was chosen as the barrier-forming polymer because of its wide application as an enteric coating material and thermoplastic properties. The influence of type and quantity of plasticizer on the processability of the polymeric formulation and the characteristics of the product were investigated. Capsular containers were obtained able to remain intact for 2 h in acidic fluids (pH 1.2) but unable to release their contents within 2 h in phosphate buffer pH 6.8, arising the need to shorten the device opening time. With this aim, release modifiers with a potential channeling action were considered.

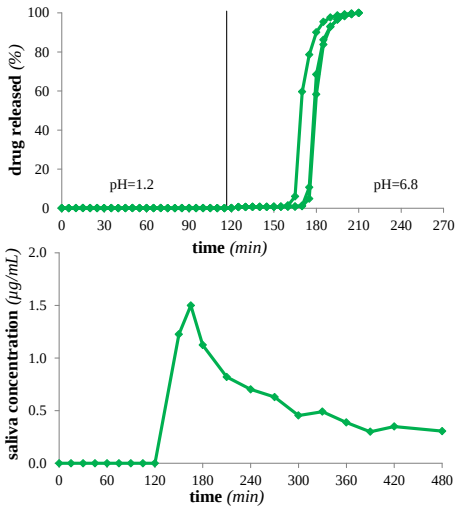

Figure 4 *in vitro* (top) and *in vivo* (bottom) performance of HPMCAS-based gastroresistant capsular containers containing Explotab® CLV [4,5]

The most encouraging results were obtained by adding a superdisintegrant to the polymeric formulation, that decreased to 30 minutes the time for complete *in vitro* dissolution/disintegration of the shell. *In vitro* and preliminary *in vivo* data relevant to systems containing Explotab® CLV (30 % by weight with respect to the plasticized polymer) are reported in Fig. 4. In particular for the *in vivo* performance promising results were obtained in terms of opening time: when compared with conventional enteric-coated capsules an only 35 minutes longer latency was noticed.

Prolonged-release container. In order to achieve a diffusion barrier for the capsule contents an insoluble but permeable polymer should be identified for the IM process. EC, plasticized with TEC, demonstrated the adequate characteristics in terms of workability and mechanical performance; on the other hand a too slow release rate of a soluble tracer was highlighted, setting up the need for increasing the shell barrier permeability (reducing the thickness or improving the porosity). A screening study on channeling agents was undertaken taking soluble components (both high melting powders of different dimensions or polymeric ones) or swelling agents (both disintegrants or swelling hydrophilic polymers) into account. Preliminary results are reported in Fig. 5 relevant to capsules containing a low viscosity grade HPC up to 50 % by weight with respect to the plasticized polymer.

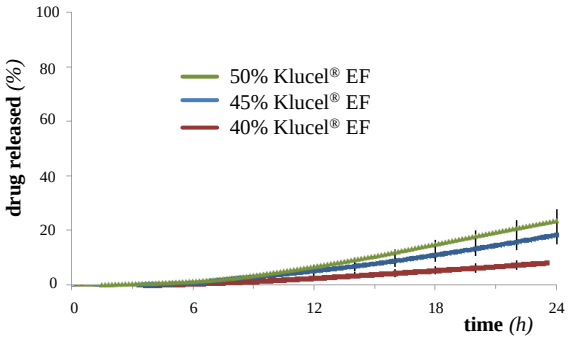

Figure 5 *in vitro* performance of EC-based prolonged-release capsular containers

Conclusion

The feasibility of injection micromolding technique for the production of oral delivery platforms allowing different release performances based on their polymeric composition was demonstrated. Capsular containers were prepared, of different size and shape, that represent an alternative configuration to traditional *reservoir* systems where the release-controlling polymeric barrier/film is transformed into a separate container shell to be filled with active principles/preparations. A step forward in the development of enteric-soluble, pulsatile/delayed and prolonged-delivery platforms was made.

References

[1] Zema L. et al., J Control Release, 159, 324-331 (2012).
[2] Gazzaniga A. et al., AAPS Pharm Sci Tech, 12, 295-303 (2011).
[3] Gazzaniga A. et al., 38th Annual Mtg & Exp CRS, 2011.
[4] Zema L. et al., Int J Pharm, 440, 264-272 (2013).
[5] Zema L. et al., 40th Annual Mtg & Exp CRS, 2013.

Session Information

All posters must be displayed for the duration of the assigned poster session. Presenting authors must be available during the presentation time to answer question and participate to discussion.

Location: Sale Rettorrato, University of Pavia

Via Strada Nuova, 65

Session 1 (poster from 1 – 15):

Exposition from 2:00 pm of November 21st to 1:30 pm of November 22nd

Thursday, November 21st 6:20 – 7:30 pm Oral presentation of posters in Aula Scarpa

Friday, November 22nd 10:45 am – 11:10 am Poster exposition in Sala Rettorato

Session 2 (poster from 16 – 30):

Exposition form 2:00 pm of November 22nd to 7:00 pm of November 23rd

Friday, November 22nd 12:50 pm – 1:30 pm Oral presentation of posters in Aula Scarpa

Friday, November 22nd 4:10 pm – 4:40 pm Poster exposition in Sala Rettorato